and interference with calcium homeostasis (24). Subjeck's group has performed extensive research and shown that the ORP150 induces antitumor immunity in vivo (25–28). Vaccination with ORP150 purified from tumors suppresses the same tumor growth in mice and induces tumor-specific CTLs. Furthermore, it has been demonstrated that ORP150 induces efficient cross-presentation of chaperoned Ags, thereby stimulating the Ag-specific CTLs (28). Moreover, the receptor for ORP150 has been shown to be SR-A and SREC-I (20). However, the precise intracellular mechanism for cross-presentation of ORP150-peptide complexes is not well understood.

In this study, we first examined whether an ORP150-precursor peptide complex could elicit a strong peptide-specific CTL response and antitumor immunity through cross-presentation using bone marrow-derived DCs (BMDCs) as APCs. Furthermore, we analyzed the intracellular trafficking pathway of the ORP150-peptide complex for efficient cross-presentation within DCs. Recently, Lakadamyali et al. have shown that early endosomes are comprised of two distinct populations, called "static" early endosome, which is slow maturing, and rapidly maturing "dynamic" early endosome (29). Furthermore, Burgdorf et al. have demonstrated that the mannose receptor introduced OVA specifically into an $EEA1^+$, $Rab5^+$-static early endosomal compartment for subsequent cross-presentation. In contrast, pinocytosis conveyed OVA to lysosome for class II presentation (30). Our observations revealed that targeting of the ORP150-peptide complex to the $EEA1^+$, $Rab5^+$-static early endosome is crucial for cross-presentation. We propose that the static early endosome plays an important role in HSP-mediated cross-presentation by DCs.

Materials and Methods

Mice

Female B6C3F1 (H-$2^{b/k}$) mice, C57BL/6 (H-2^b) mice, and $TAP1^{-/-}$ (H-2^b) mice were purchased from The Jackson Laboratory and used at 6 wk of age. Mice were maintained in a specific pathogen-free mouse facility at Sapporo Medical University according to institutional guidelines for animal use and care.

Cells

The B3Z cell is a $CD8^+$ T cell hybridoma specific for the $OVA_{258-265}$ epitope (SL8) in the context of H-$2K^b$. The KZO cell is a $CD4^+$ T cell hybridoma specific for the $OVA_{247-265}$ (PL19) in the context of I-A^k. These hybridomas synthesize a reporter enzyme when the TCR engages the H-$2K^b$-SL8 (SIINFEKL) complex or the I-A^k-PL19 (PDEVSGLEQLESI INFEKL) complex, respectively. The cell lines were obtained from Dr. N. Shastri (University of California at Berkeley, Berkeley, CA). RMA-S-A*2402 cells were RMA-S transfected with the gene encoding HLA-A*2402 (provided by Dr. H. Takasu, Dainippon-Sumitomo Pharmaceutical, Osaka, Japan). TG3 cells are a methylcholanthrene-induced fibrosarcoma derived from the HLA-A*2402 transgenic mouse. TG3–2B cells were TG-3 transfected with the gene encoding human survivin-2B. YAC-1 cells and 293T cells were obtained from the American Type Culture Collection.

Generation of BMDCs

Bone marrow-derived immature DCs were generated from bone marrow cells that were obtaind from the femurs and tibiae of female C57BL/6 mice, B6C3F1 mice, and $TAP^{-/-}$ mice. Bone marrow cells (1×10^4/well) in a 24-well plate were cultured in complete RPMI 1640 with 10% FCS and 20 ng/ml GM-CSF (Endogen) for 5 days. Medium with GM-CSF was gently replaced on day 2 and day 4.

Construction of secreted form of ORP150 and generation of 293T cells secreting ORP150

Using human ORP150 cDNA as a template, the sense primer (5′CGG GATCCATGGCAGACAAAGTTAGGAGG-3′) and the antisense primer (5′-GGACAGAAGCGGCCTTTGAAGGCGGCCGCCG-3′) were used to generate an $NDEL^-$ ORP150 cDNA. The PCR product was digested with *Bam*HI/*Not*I and ligated into pIRESpuro3-myc/His vector (Clontech Laboratories). The sequence of the construct was verified by DNA sequencing. 293T cells were transfected with this construct using Lipofectamine 2000 (Invitrogen). Cells were then subcloned with 1 mg/ml puromycin (Invitrogen) and a 293T cell-secreting ORP150, 293T-ORP4, was established.

Purification of secreted ORP150

293T-ORP4 cells were cultured with 10% DMEM for 3 days. Then, the culture supernatant of 293T-ORP4 cells was collected and applied to a Con A-agarose column (Amersham Biosciences). After extensive washing of the column with Con A-PBS (150 mM NaCl, 5 mM NaP, 1.35 mM KCl, 1.35 mM $MgCl_2$), ORP150 was eluted off with Con A-PBS containing 10 mM methyl α-D-mannopyranoside (Sigma-Aldrich). The presence of ORP150 in the eluted fraction was examined by SDS-PAGE stained with Coomassie brilliant blue (Bio-Rad) and Western blotting using a mAb against ORP150 (IBL). Typically, fractions 2–5 contained purified ORP150 and these fractions were pooled and concentrated using Microcon YM-100 (Millipore). The concentration of ORP150 was determined using a Micro BCA protein assay reagent kit (Pierce). Quantification of the endotoxin in the purified ORP150 was performed using the endotoxin-specific chromogenic test (ES test; Seikagaku Kogyo). If the endotoxin in the ORP150 preparation was higher than the limit of detection (<5 pg/ml), endotoxin was depleted using Detoxi-Gel endotoxin removing gel (Pierce) and then requantified.

Peptides and proteins

The following peptides were used (underlined sequences represent the precise MHC class I- or class II-binding epitope): survivin-$2B_{80-88}$ (AYACNTSTL), SL8 (SIINFEKL), SL8C (SIINFEKLTEWTS), PL19 (PDEVSGLEQLESIINFEKL), PLC24 (PDEVSGLEQLESIINFEKLTEWTS), and SLC26 (SIINFEKLTEWTSSNVMEERKIKVYL). All peptides were synthesized on a solid phase support using F-moc for transient NH_2-terminal protection and were characterized using mass spectrometry. They were purified by HPLC to >99% homogeneity and stored at 2 mM in distilled H_2O at −80°C. BSA was purchased from Sigma-Aldrich. Chicken OVA was purchased from Calbiochem and stored at 20 mg/ml in PBS at −80°C.

Antibodies

Confocal laser microscopy was used to detect organelles with specific Abs: an anti-Rab5 pAb (MBL) and EEA1 (Abcam) for early endosomes, anti-lysosome-associated membrane protein 1 (LAMP-1) pAb (Santa Cruz Biotechnology) for late endosomes/lysosomes, anti-Rab11 pAb (Santa Cruz Biotechnology) for recycling endosomes, and anti-KDEL mAb (StressGen Biotechnologies) for ER. mAb 25D-1.16 specific for the $K^b/OVA_{257-264}$ complexes was provided by Dr. R. Germain (National Institutes of Health, Bethesda, MD). The Abs were each conjugated with Alexa Fluor 488 (Molecular Probes) according to the manufacturer's instructions. Alexa Fluor 594 (Molecular Probes) was used for labeling ORP150.

Generation of ORP150-peptide complex in vitro

Peptide SLC26 (SIINFEKLTEWTSSNVMEERKIKVYL) was iodinated with ^{125}I using IODO-BEADS (Pierce) according to the manufacturer's instructions. ORP150 or control protein BSA was mixed with the ^{125}I-labeled peptide in a 50:1 peptide-to-protein molar ratio in 0.7 M NaCl containing sodium-phosphate buffer and heated at 45°C for 30 min, then incubated for 30 min at room temperature. The complex was separated from unbound peptide using a Microcon YM-100 or YM-30 (Millipore). Radioactivity of the complex and unbound peptide was measured in a gamma counter for evaluation of the binding efficiency of the ORP-peptide complex. Samples were then analyzed by SDS-PAGE, followed by autoradiography of the stained gel.

In vitro cross-presentation assay

DCs (1×10^5) from C57BL/6 or $TAP^{-/-}$ mice were pulsed with PLC24 (20 μg) alone, different ORP150/peptide dose ratios, or SL8 (1 μM) for 2 h at 37°C in 100 μl of Opti-MEM, and fixed for 1 min with 0.01% glutaraldehyde. Fixation was stopped by addition of 2 M L-lysine and the cells were washed twice with RPMI 1640 medium and cultured overnight with 1×10^5 B3Z. The B3Z response was measured as β-galactosidase activity induced upon ligand recognition. The β-galactosidase activity was measured by the absorbance at 595 nm of the cleavage product of chlorophenol red-β-D-galactopyranoside (CPRG; purchased from Roche). In other experiments, DCs (1×10^5) from C57BL/6 or $TAP^{-/-}$ mice were pulsed with ORP150 (20 μg) alone, PLC24 (20 μg) alone, a complex of both generated in vitro, a simple mixture of both, OVA (200 μg/ml), or SL8 (1 μM) for 2 h at 37°C in 100 μl of Opti-MEM, fixed, and then cocultured overnight with 1×10^5 B3Z.

Ag presentation assay

DCs (1×10^5) from B6C3F1 mice were pulsed with ORP150 (20 μg) alone, PLC24 (20 μg) alone, a complex of both generated in vitro, a simple mixture of both, OVA (200 μg/ml), or PL19 (1 μM) for 2 h at 37°C in 100 μl of Opti-MEM, and fixed for 1 min with 0.01% glutaraldehyde. Fixation was stopped by addition of 2 M L-lysine and the cells were washed twice with RPMI 1640 medium and cultured overnight with 1×10^5 KZO. The KZO response was measured as β-galactosidase activity using CPRG by the absorbance at 595 nm.

In vivo cross-presentation assay

C57BL/6 mice were immunized in their footpads with ORP150 (50 μg) alone, SL8C (50 μg) alone, or the ORP150 (50 μg)-SL8C (50 μg) complex. Draining popliteal lymph nodes were removed after 12 h, and $CD11c^+$ DCs were purified using CD11c MACS beads (Miltenyi Biotec). Purified DCs were plated at a density of $1 \times 10^3/200$ μl in 10% RPMI 1640 and cocultured overnight with 1×10^5 B3Z. Stimulated B3Z cells were stained with CPRG and red color was measured as absorbance at 595 nm.

Inhibition studies

DCs (1×10^5) from B6C3F1 mice were preincubated with primaquine (ICN Biomedicals). Primaquine was not toxic in our culture systems. Two hours after preincubation, the DCs were pulsed with the ORP150 (20 μg)-PLC24 (20 μg) complex, SL8 (1 μM), or PL19 (1 μM) for 2 h at 37°C in 100 μl of Opti-MEM, then fixed, washed, and cultured overnight with B3Z or KZO. Stimulated B3Z or KZO were stained with CPRG and red color was measured as absorbance at 595 nm.

Immunocytological localization of ORP150-SL8C complex

ORP150, transferrin (Molecular Probes), and OVA were conjugated with Alexa Fluor 594 (Molecular Probes) according to the manufacturer's instructions. Immature BMDCs were incubated at 37°C with Alexa Fluor 594-labeled ORP150 (20 μg) complexed with PLC24 (20 μg) for 1 h. Following incubation, cells were washed twice with ice-cold PBS and fixed with ice-cold acetone for 1 min. Organelles were stained with an anti-Rab5 pAb and EEA1 mAb for early endosomes, anti-LAMP-1 pAb for late endosomes and lysosomes, anti-Rab11 pAb for recycling endosomes, or anti-KDEL mAb for ER, followed by Alexa 488-conjugated goat anti-rabbit IgG or anti-mouse IgG and visualized with a Bio-Rad MRC1024ES confocal scanning laser microscope system. For detecting the intracellular localization of H-$2K^b$/SL8 complex using mAb 25D-1.16, the DCs were first incubated with ORP150 complexed with PLC24 for 1 h and fixed with cold acetone. DCs were then incubated with anti-mouse CD16/CD32 Fc-block to block nonspecific staining, followed by costaining with an Alexa Fluor 594-labeled mAb 25D1.16 and anti-organelle Abs conjugated with Alexa Fluor 488. For evaluation of colocalization, single z-plane of one cell was evaluated. For each protein and organelle combination, a total of 90 cells (30 cells from three independent experiments) were analyzed.

^{51}Cr-release assay

Each HLA-A*2402/K^b transgenic mouse was immunized s.c. at the base of the tail, twice with a 1-wk interval, with the ORP150 (50 μg)-survivin-2B peptide (50 μg) complex. One week after the last immunization, splenocytes of immunized mice were cultured with irradiated (100 Gy) and survivin-$2B_{80-88}$ peptide-pulsed naive spleen cells for 5 days. Subsequently, the generation of survivin-$2B_{80-88}$ peptide-specific CTLs was evaluated in a ^{51}Cr-release assay. The specificity of CTLs induced was evaluated using TG3–2B cells, RMA-S-A*2402 cells, RMA-S-A*2402 cells pulsed with 1 μg/ml survivin-$2B_{80-88}$ peptide, and YAC-1 cells as targets.

Transplantation of tumor cells and immunotherapy

TG3–2B cells (5×10^5) were intradermally transplanted into the right flank in HLA-A*2402/K^b transgenic mice on day 0. When average tumor diameter reached 3–4 mm, the mice were then treated with ORP150 (50 μg) alone, the ORP150 (50 μg)-survivin-$2B_{80-88}$ peptide (50 μg) complex, or survivin-$2B_{80-88}$ peptide (50 μg) via s.c. administration at the nape of the neck twice each week for 2 wk (on days 9, 12, 17, and 21). Control groups of mice were immunized with PBS. Tumor growth was recorded twice each week. Average diameters of the two axes were plotted so that therapeutic effects could be compared among the groups. On day 35, tumor rejection rates were compared among the groups. Average tumor diameters on day 28 were statistically analyzed using the Mann-Whitney U test. Statistical analyses for evaluating the survival advantages were performed using log-rank analysis. All of the experiments were performed with 8–10 mice per group.

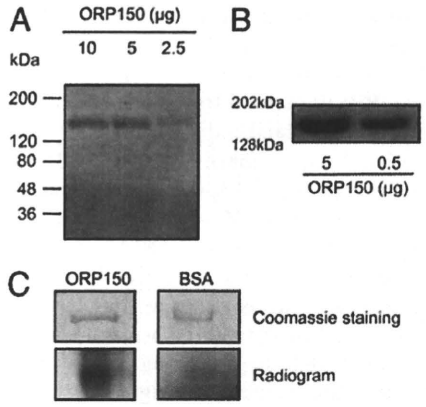

FIGURE 1. Purification of secreted form of ORP150. *A*, Purified ORP150 (10, 5, or 2.5 μg) was analyzed by SDS-PAGE and stained using Coomassie brilliant blue, followed by (*B*) Western blotting using a mAb against ORP150. *C*, ORP150 and BSA were mixed with a ^{125}I-labeled peptide in a 50:1 peptide-to-protein molar ratio in sodium phosphate buffer. Samples were analyzed by SDS-PAGE and stained using Coomassie brilliant blue, followed by autoradiography of the stained gel.

Immunohistochemical analysis

After treatment of the preestablished TG3–2B tumor with the ORP150-survivin-2B peptide complex or PBS, tumor tissue was excised on day 35. The frozen tissues were stained with an anti-mouse CD4 mAb (Santa Cruz Biotechnology) or an anti-mouse CD8 mAb (Chemicon International) and then incubated with HRP-conjugated goat anti-rat Ig (Dako), followed by hematoxylin counterstaining. The numbers of tumor-infiltrating $CD4^+$ and $CD8^+$ T cells were counted in 10 high-power fields (HPF; ×400).

Statistical analysis

All experiments except for the tumor transplantation experiments were independently performed three times in triplicate. Results were given as means SEM. Comparisons between two groups were performed using Student's t test, whereas comparisons between multiple groups were done using ANOVA test, with a value of $p < 0.05$ considered to be statistically significant.

Results

Purification of secreted form of ORP150

Secreted ORP150 was purified from the culture supernatant of 293T-ORP4 cells using a Con A-Sepharose column as described in *Materials and Methods*. Fractions containing homogeneous ORP150 were collected and characterized by gel staining (Fig. 1*A*) and immunoblotting using a mAb to ORP150 (Fig. 1*B*). This revealed the homogeneity of ORP150 preparations with little contamination from other proteins. To critically evaluate the capacity of ORP150 to elicit immune responses, we carefully removed endotoxin that can activate innate immune responses. The purified ORP150 did not affect the cell surface expression of MHC class I molecules, MHC class II molecules, CD80, and CD86 of DCs, indicating the inability of ORP150 for DC maturation (data not shown). Additionally, DCs pulsed with the purified ORP150 did not stimulate the production of TNF-α or IL-12, also indicating minimal or no endotoxin in the purified ORP150 (data not shown).

Generation of ORP150-peptide complex in vitro

We ascertained and quantified the loading of peptides onto ORP150. We employed the iodinated SLC26 peptide as a tracer. As others and as we have already demonstrated, heat shock treatment accelerates the loading of peptides onto the binding sites of ORP150 and other HSPs (22). As shown in Fig. 1*C*, ORP150 bound labeled peptides efficiently, but control protein BSA bound

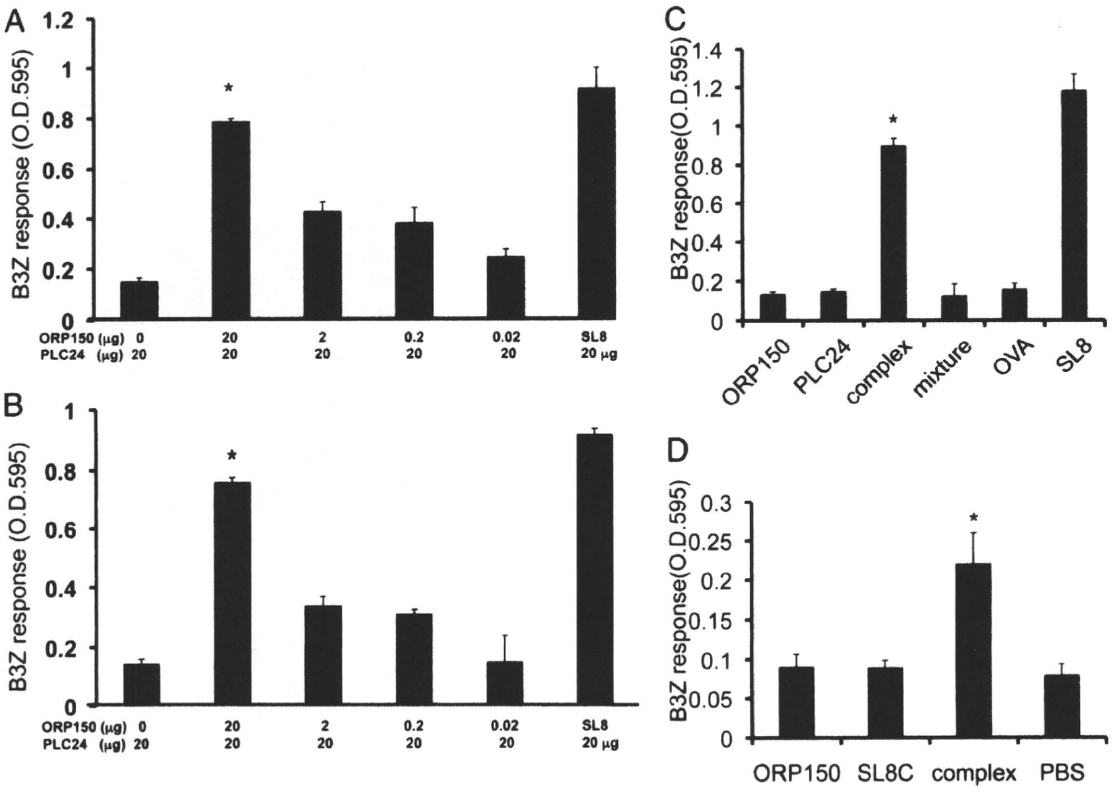

FIGURE 2. Cross-presentation of ORP150-chaperoned peptides by BMDCs in vitro and vivo. *A* and *B*, DCs (1×10^5) from C57BL/6 mice were pulsed with PLC24 (20 μg) alone, different ORP150/peptide dose ratios, or SL8 (1 μM) for 2 h at 37°C in 100 μl of Opti-MEM, and fixed for 1 min with 0.01% glutaraldehyde. *C*, ORP150 alone, PLC24 alone, a complex of both, a mixture of both, OVA, or SL8 was loaded onto BMDCs and cultured overnight with B3Z. The B3Z response was analyzed using CPRG. *D*, B6C3F1 mice were immunized into the footpads with ORP150 alone, SL8C alone, or a complex of both. After 12 h, $CD11c^+$ DCs were isolated from draining popliteal lymph nodes and cocultured with B3Z. The B3Z response was analyzed using CPRG. Data are shown as means ± SEM of three independent experiments. *, $p < 0.01$.

only marginal levels. The molar ratio of the bound SLC26 peptide to ORP150 was 3.95 mol of peptide per mole of ORP150 protein.

ORP150-PLC24 peptide complex is cross-presented by DCs in vitro and vivo

We first examined whether ORP150 facilitated the cross-presentation of the chaperoned precursor peptide. To determine the optimal ORP150/peptide dose ratio, DCs from C57BL/6 mice were loaded with different ORP150/peptide dose ratios for 2 h, fixed, and then cocultured with B3Z $CD8^+$ T cell hybridoma. As shown in Fig. 2, *A* and *B*, we observed that the complex generated using 20 μg/ml ORP150 and 20 μg/ml PLC24 peptide yielded sufficiently enough for the cross-presentation. In contrast, the same dose of PLC24 peptide alone was not cross-presented by DCs. Additionally, we examined whether complex formation between ORP150 and peptide was required for enhanced cross-presentation. DCs were pulsed with ORP150 alone, the PLC24 precursor peptide alone, a complex of both generated in vitro, a simple mixture of both, OVA protein, or SL8 peptide (for positive control) for 2 h at 37°C, then fixed, washed, and cultured with B3Z. The ORP150-PLC24 peptide complex elicited a strong B3Z response, while ORP150 alone, PLC24 peptide alone, or a simple mixture of both did not induce a B3Z response (Fig. 2*C*). Thus, the presence of ORP150 did not enhance the cross-presentation of uncomplexed PLC24 precursor peptide. These results indicated that cross-presentation of OVA-derived peptide was enhanced only if exogenous precursor peptide was complexed to the ORP150. Additionally, soluble OVA was not cross-presented at the concentration used (200 μg/ml) in this study (Fig. 2*C*). Furthermore, we examined whether cross-presentation of the ORP150-peptide complex occurred in vivo. We immunized B6C3F1 mice with the ORP150-SL8C complex, SL8C alone, or ORP150 alone and evaluated the appearance of $CD11c^+$ DCs that could stimulate B3Z in the draining lymph nodes (Fig. 2*D*). $CD11c^+$ DCs from mice immunized with the ORP150-SL8C complex elicited a significant B3Z response.

ORP150-peptide complex also facilitates Ag presentation to $CD4^+$ T cells

As the PLC24 peptide included both the H-$2K^b$ epitope SL8 and I-A^k epitope PL19, we tested whether the ORP150-PLC24 peptide complex was presented through the MHC class II pathway, thereby inducing $CD4^+$ T cell responses. DCs from B6C3F1 mice were pulsed with ORP150 alone, PLC24 peptide alone, a complex of ORP150 and PLC24 peptide, a simple mixture of both, soluble OVA, or PL19 peptide (for positive control) for 2 h at 37°C, then cells were fixed, washed, and cocultured with KZO $CD4^+$ T cell hybridoma. While ORP150 alone and the PLC24 peptide alone were unable to induce $CD4^+$ T cell responses, the ORP150-PLC24 peptide complex induced a robust $CD4^+$ T cell response as well as a $CD8^+$ T cell response (Fig. 3). As expected, soluble OVA was also presented in association with I-A^k. These data indicated that a cross-presentation competent "ORP150-peptide complex" and incompetent "soluble OVA" might be translocated to different intracellular compartments for Ag processing and presentation. Based on our observation, we focused on the intracellular trafficking mechanism responsible for ORP150-mediated cross-presentation compared with soluble OVA.

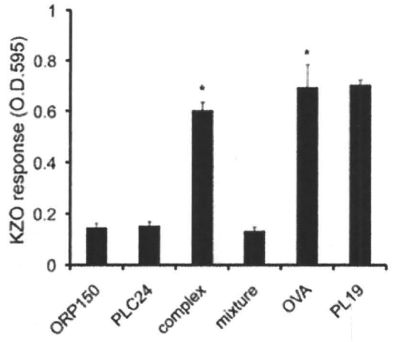

FIGURE 3. Ag presentation through MHC class II pathway in vitro. ORP150 alone, PLC24 alone, a complex of both, a mixture of both, OVA, or PL19 peptide was loaded onto BMDCs from B6C3F1 mice, which were cultured overnight with KZO. The KZO response was analyzed using CPRG. Data are shown as means ± SEM of three independent experiments. *, $p < 0.01$.

ORP150-PLC24 peptide complexes are cross-presented by a TAP-independent and recycling pathway

It is generally accepted that exogenous Ags are cross-presented by two distinct pathways in a TAP-dependent and -independent fashion. We examined whether cross-presentation of the ORP150-PLC24 peptide complex depended on TAP transport. DCs from B6C3F1 or $TAP^{-/-}$ mice were pulsed with the ORP150-PLC24 complex for 2 h. DCs from the $TAP^{-/-}$ mouse could process and present the ORP150-chaperoned peptide as efficiently as did DCs from the wild-type mouse (Fig. 4*A*). This suggested that ORP150-mediated cross-presentation might involve an endosome-recycling pathway. Therefore, we used primaquine, an inhibitor of membrane recycling, in the cross-presentation assay. DCs were preincubated with primaquine and subsequently pulsed with the ORP150-PLC24 complex. Primaquine did, indeed, show the dose-dependent inhibition of cross-presentation of the ORP150-chaperoned peptide (Fig. 4*B*). These data suggested that cross-presentation of the ORP150-PLC24 complex accessed recycling MHC class I molecules in endocytic compartments.

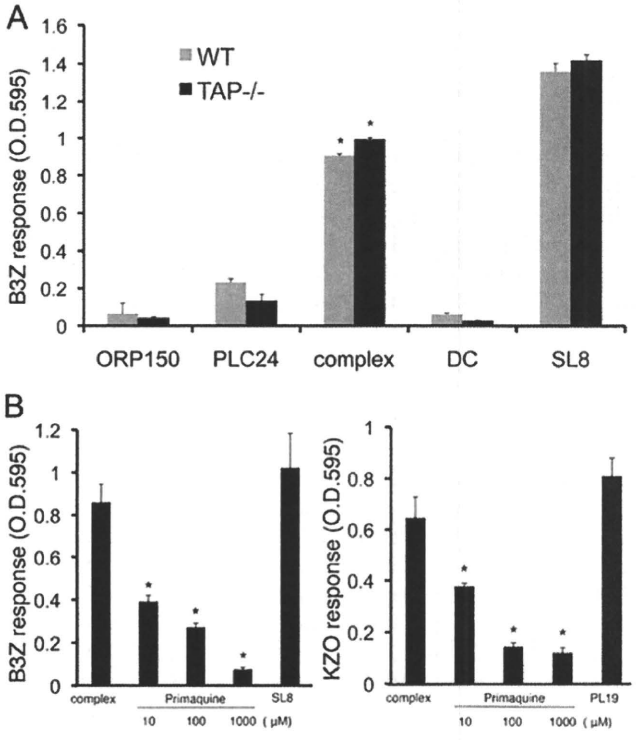

FIGURE 4. The ORP150-PLC24 peptide complex is cross-presented by TAP-independent pathway. *A*, BMDCs from B6C3F1 (wild type, WT) or $TAP^{-/-}$ mice were pulsed with ORP150 alone, PLC24 alone, a complex of both, or SL8. The DCs were then fixed, washed, and cultured overnight with B3Z. The B3Z response was analyzed using CPRG. *B*, DCs from B6C3F1 mice were preincubated with indicated concentrations of primaquine. The DCs were then pulsed with the ORP150-PLC24 complex or PL19 for 2 h. The B3Z response was analyzed using CPRG. Data are shown as means ± SEM of three independent experiments. *, $p < 0.01$.

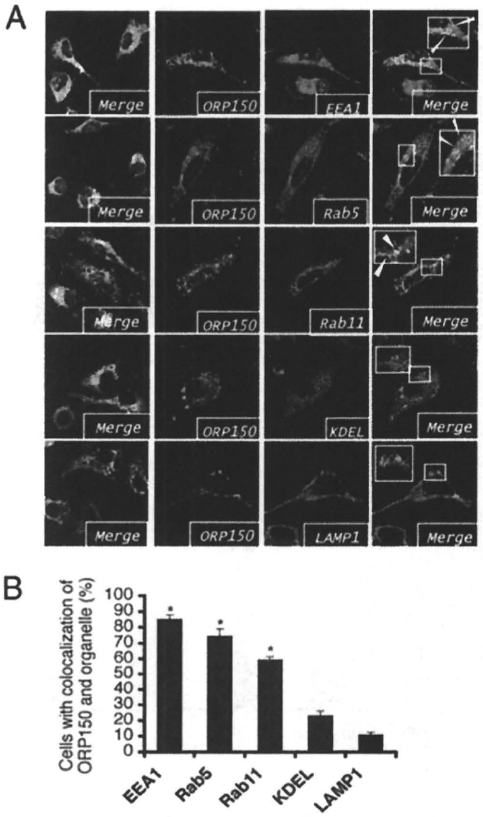

FIGURE 5. Intracellular localization of ORP150-PLC24 complex. *A*, BMDCs were incubated at 37°C with an Alexa Fluor 594-labeled ORP150-PLC24 complex for 1 h, then washed and fixed. Organelles were stained with an anti-EEA1 mAb for early endosomes, anti-Rab5 pAb for early endosomes, anti-Rab11 pAb for recycling endosomes, anti-KDEL mAb for ER, and anti-LAMP-1 pAb for late endosomes/lysosomes, followed by Alexa Fluor 488-conjugated goat anti-rabbit IgG or anti-mouse IgG and visualized with confocal laser microscopy. Colocalization of the internalized ORP150-peptide complex and each organelle is indicated with arrows. *B*, To quantify the percentage of the colocalization, a single *z*-plane of one cell was evaluated. For each protein and organelle combination, a total of 90 cells (30 cells from three independent experiments) were analyzed. Data are shown as means ± SEM of three independent experiments. *, $p < 0.01$.

Immunocytological localization of ORP150-PLC24 peptide complex

To further support all of the above results, we investigated the intracellular routing of ORP150 after uptake of it in DCs, using confocal laser microscopy. DCs were incubated with the Alexa Fluor 594-labeled ORP150-PLC24 peptide complex for 1 h. Following incubation, the cells were fixed and stained with Abs against markers for organelle structures such as EEA1, Rab5, LAMP-1, Rab11, and KDEL. The Alexa Fluor 594-labeled ORP150-peptide complex was detected in $EEA1^+$, $Rab5^+$-early endosomes and $Rab11^+$-recycling endosomes, but not in lysosomes or ER (Fig. 5*A*). Quantitative analysis of the colocalization between the exogenous ORP150-peptide complex and EEA1,

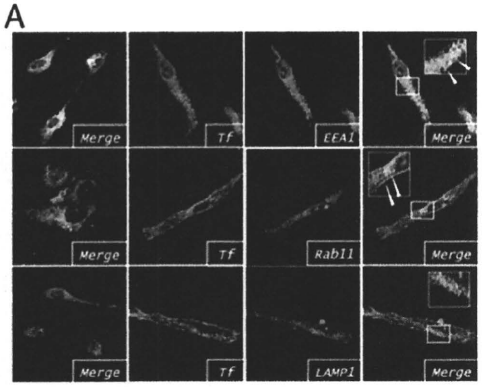

FIGURE 6. *A*, DCs were incubated at 37°C with Alexa Fluor 594-labeled transferrin (Tf). Organelles were stained with an anti-EEA1 mAb, anti-Rab5 pAb, anti-Rab11 pAb, and anti-LAMP-1 pAb, followed by Alexa Fluor 488-conjugated goat anti-rabbit IgG or anti-mouse IgG. Colocalization of internalized transferrin and each organelle is indicated with arrows. *B*, To quantify the percentage of the colocalization, a single *z*-plane of one cell was evaluated. For each protein and organelle combination, a total of 90 cells (30 cells from three independent experiments) were analyzed. Data are shown as means ± SEM of three independent experiments. *, $p < 0.01$.

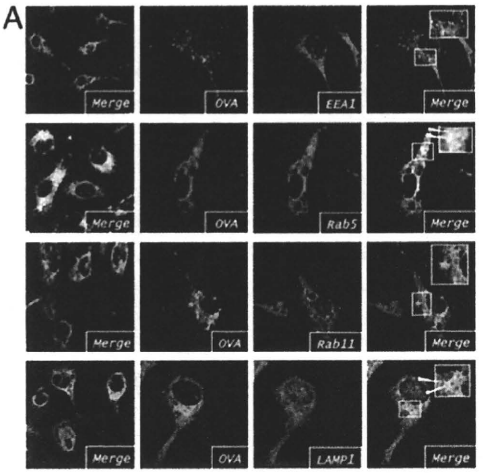

FIGURE 7. *A*, DCs were incubated at 37°C with Alexa Fluor 594-labeled OVA. Organelles were stained with an anti-EEA1 mAb, anti-Rab5 pAb, anti-Rab11 pAb, and anti-LAMP-1 pAb, followed by Alexa Fluor 488-conjugated goat anti-rabbit IgG or anti-mouse IgG. Colocalization of internalized OVA and each organelle is indicated with arrows. *B*, To quantify the percentage of the colocalization, a single *z*-plane of one cell was evaluated. For each protein and organelle combination, a total of 90 cells (30 cells from three independent experiments) were analyzed. Data are shown as means ± SEM of three independent experiments. *, $p < 0.01$.

Rab5, and Rab11 revealed an average colocalization incidence of 85.6, 74.4, and 58.9%, respectively, further evidencing that the exogenous ORP150-peptide complex was delivered to an endosome-recycling pathway (Fig. 5*B*). Moreover, we examined the dynamics of Alexa Fluor 594-labeled transferrin as a positive control protein for recycling endosomes (Fig. 6). As expected, transferrin localized to $EEA1^+$-static early endosomes and $Rab11^+$-recycling endosomes. In contrast, Alexa Fluor 594-labeled soluble OVA localized to the $Rab5^+$ early endosome as well as the $LAMP\text{-}1^+$ late endosome/lysosome, but not to the $EEA1^+$ or $Rab11^+$ compartment, thus indicating the dynamic endosomal pathway (Fig. 7). These results indicated that the ORP150-peptide complex was sorted into the static endosomal pathway, not the dynamic endosomal pathway. In contrast, the soluble OVA protein, which was not cross-presented, was translocated to the dynamic endosomal pathway. These data suggested that targeting to the static early endosome was required for efficient cross-presentation by DCs.

Early endosomes and recycling endosomes are the compartments where exogenous ORP150-chaperoned precursor peptides are processed and transferred onto recycling MHC class I molecules

To investigate in which compartment the ORP150-PLC24 peptide complex was processed and resulting peptide bound to MHC class I molecule, we used mAb 25D1.16, as this mAb recognized the SL8 peptide-H-$2K^b$ complex. We clearly observed that mAb 25D1.16 was detected in early endosome and recycling endosome, and not in the ER (Fig. 8). To confirm the staining specificity of mAb 25D1.16, DCs were incubated with ORP150-irrelevant peptide survivin-$2B_{80-88}$ complex and examined the colocalization of mAb 25D1.16 and each organelle. We did not observe the specific staining of mAb 25D1.16 (supplemental Fig. 1).[4] These data indicated that the ORP150-chaperoned precursor peptides were processed and bound to MHC class I within early endosomes and recycling endosomes, suggesting that recycling MHC class I molecules were necessary for efficient cross-presentation of the ORP150-chaperoned peptides.

Potent antitumor effect of immunization with ORP150-peptide complex against established tumor

HLA-A*2402/K^b transgenic mice are a well-established model for studying HLA-A*2402-restricted CTL epitopes and vaccine development (31). We previously reported survivin-2B as a universal tumor Ag and identified an HLA-A24-restricted antigenic peptide, survivin-$2B_{80-88}$ (AYACNTSTL), recognized by $CD8^+$ CTLs (32). We therefore examined the efficacy of ORP150-based immunotherapy using human tumor Ag survivin-2B as a surrogate Ag. HLA-A*2402/K^b transgenic mice were inoculated with methylchoranthrene-induced fibrosarcoma TG3 transfected with survivin-2B cDNA, TG3–2B. When tumor diameter reached 3–4 mm, treatment with s.c. injection of an ORP150-survivin-2B complex, ORP150 alone, survivin-2B peptide alone, or PBS was conducted (Fig. 9*A*). As shown in Fig. 9*B*, the growth of established TG3–2B tumors was significantly retarded in the group treated with the ORP150-survivin-2B complex compared with survivin-2B peptide alone, ORP150 alone, and PBS (vs survivin-2B, $p = 0.027$; vs ORP150, $p = 0.016$; vs PBS, $p = 0.0002$). We also

[4] The online version of this article contains supplemental material.

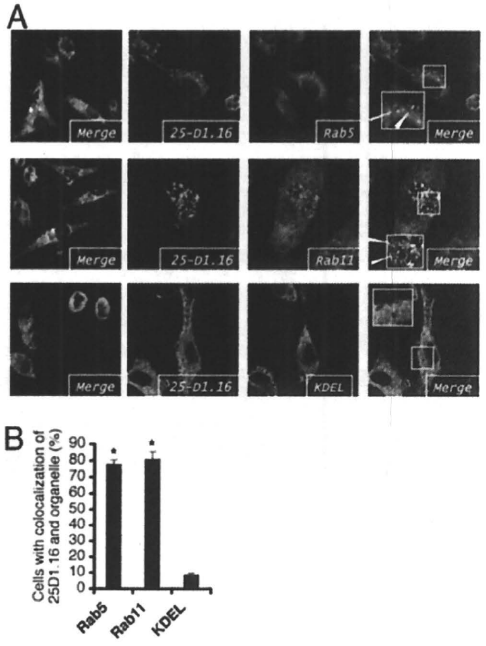

FIGURE 8. *A*, DCs were first incubated with ORP150 complexed with PLC24 for 1 h and fixed with cold acetone. DCs were then incubated with anti-mouse CD16/CD32 Fc-block to block nonspecific staining, followed by costaining with an Alexa Fluor 594-labeled mAb 25D1.16 and anti-organelle Abs conjugated with Alexa Fluor 488. Colocalization of H-2K^b/SL8 complex and each organelle are indicated with arrows. *B*, For evaluation of colocalization, a single *z*-plane of one cell was evaluated. For 25D1.16 and each organelle combination, a total of 90 cells (30 cells from three independent experiments) were analyzed. Data are shown as means ± SEM of three independent experiments. *, $p < 0.01$.

evaluated the tumor rejection rates for the ORP150-survivin-2B peptide complex and compared with survivin-2B peptide alone, ORP150 alone, and PBS (vs survivin-2B, $p = 0.070$; vs ORP150, $p = 0.048$; vs PBS, $p = 0.007$) (Fig. 9*C*). Notably, six of nine mice in the ORP150-survivin-2B complex-treated group rejected the established tumors. These data strongly suggested that immunization with the ORP150-tumor peptide complexes were an effective immunotherapeutic approach for various types of cancer expressing survivin-2B and HLA-A*2402. Next, we confirmed whether CD8$^+$ T cells infiltrated within the established tumor mass in response to immunization with the ORP150-survivin-2B complex by immunohistological analysis (Fig. 9*D*). More CD8$^+$ T cells were observed in the tumor tissues injected with complex (328 cells/10 HPF) than in the PBS control (59 cells/10 HPF). We also examined CD4$^+$ T cell infiltration. The extent of CD4$^+$ T cell infiltration in mice immunized with the ORP150-survivin-2B complex (176 cells/10 HPF) was also greater than that of mice immunized with PBS (53 cells/10 HPF). Moreover, we tested whether in mice treated with the ORP150-survivin-2B complex, survivin-2B-specific CTL responses were induced. Spleen cells of mice treated with the ORP150-survivin-2B complex showed significant cytotoxicity against TG3–2B cells and survivin-2B-coated RMA-S-A*2402 cells, but not survivin-2B-noncoated RMA-S-A*2402 cells or YAC-1 cells (Fig. 9*E*). We also examined the tetramer assay using survivin-2B-HLA-A*2402/human β_2-microglobulin tetramer (33). However, we were unable to detect apparent tetramer-positive population (data not shown). The reason for this may be attributed to the species difference of β_2-microglobulin. These results showed that the ORP150-Ag peptide complex induced a strong CTL response to the chaperoned peptide and that this response was sufficiently strong to generate antitumor effects.

Discussion

It is well demonstrated that immunization with tumor-derived HSPs or HSPs complexed with an Ag peptide/protein elicits tumor- or Ag-specific CD8$^+$ T cell responses. Above all, it has been shown that Hsp70- and gp96-Ag complexes facilitate Ag presentation in association with MHC class I molecules (16, 34, 35). However, the ability of HSPs to facilitate the presentation of MHC class II-restricted epitopes and to prime CD4$^+$ T cells has been relatively unexplored. In recent reports, it has been shown that Hsp70- and gp96-Ag complexes facilitate Ag presentation in association with both MHC class I and class II molecules (34, 36, 37). In this study, we demonstrated that ORP150-Ag complexes also facilitated Ag presentation in association with both MHC class I molecules and MHC class II molecules via an endosome-recycling pathway. In vaccine development, ORP150 has advantages for the induction of specific CTLs due to the simultaneous activation of specific helper T cells, which are required for efficient

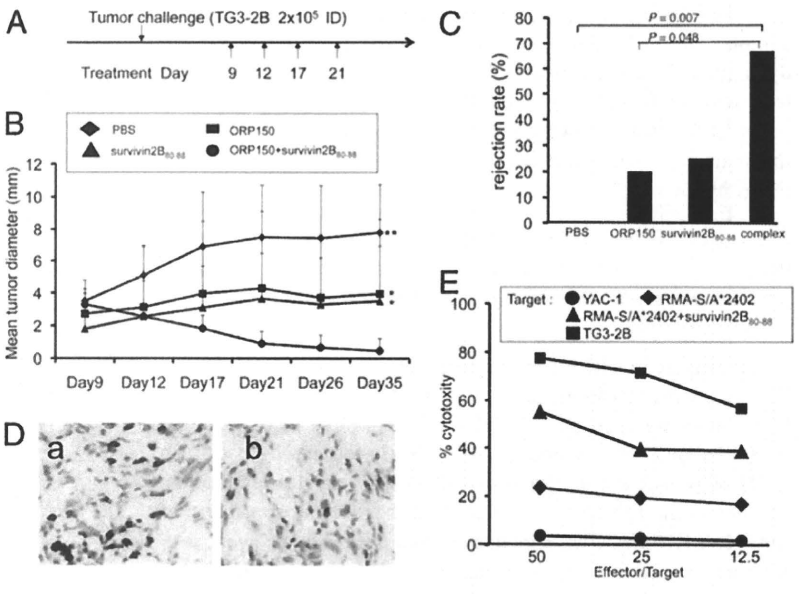

FIGURE 9. ORP150-tumor Ag peptide complexes induce strong antitumor effects. *A*, The protocol for immunotherapy is shown. *B*, A total of 2×10^5 TG3–2B cells were first injected intradermally into HLA-A*2402/K^b mice (10 animals/group). When mean tumor diameter reached 3–4 mm, mice were given the treatment with the ORP150 (50 μg)-survivin-2B$_{80-88}$ (50 μg) complex, ORP150 (50 μg) alone, survivin-2B$_{80-88}$ (50 μg) alone, or PBS twice a week. *C*, The remaining 8–10 mice in each group were observed for the tumor rejection rate. *D*, The frozen tissues excised from mice treated with (*a*) the ORP150-survivin-2B$_{80-88}$ peptide complex or (*b*) PBS control was stained with an anti-mouse CD8 mAb (×400). *E*, Immunization with the ORP150-Ag peptide complex induced peptide specific CTLs. After immunizaton with the ORP150-survivin-2B$_{80-88}$ peptide complex, splenocytes of the mice were cultured with survivin-2B$_{80-88}$ peptide for 5 days and tested for cytotoxicity. Representative data are shown as means ± SEM of three independent experiments. *, $p < 0.05$ and **, $p < 0.01$.

CTL induction. In other words, when it is required for activation of $CD8^+$ T cells as well as $CD4^+$ T cells via Ag presentation in the context of both MHC class I and class II molecules, ORP150 can be a potent enhancer in immunotherapy.

Recent studies have revealed that stressful stimuli induce active release of intracellular HSPs into the extracellular milieu. The extracellular HSPs play an important role in initiating immune responses against microbial infection and neoplastic cells (10, 38). Because virus-infected cells and tumor cells are not able to prime naive $CD8^+$ T cells due to the lack of costimulatory molecules, priming of $CD8^+$ T cells against tumor cells and virus-infected cells requires cross-presentation by APCs. Extracellular HSP-Ag complexes, which are released from damaged tumor cells or virus-infected cells, are considered to be candidate Ag sources for cross-presentation. The pathway for cross-presentation has been shown to be comprised of two distinct intracellular routes, a proteasome-TAP-dependent pathway and an endosome-recycling pathway (22, 39). Recent reports have identified the pathway wherein peptide exchange onto recycling MHC class I molecules occurs within early endosomal compartments (40). We have shown that ORP150-mediated cross-presentation is independent of TAP and sensitive to primaquine, indicating that sorting of peptides onto MHC class I occurs via an endosome-recycling pathway. Very recently, Lakadamyali et al. (29) have shown that early endosomes are comprised of two distinct populations: a dynamic population that is highly mobile on microtubules and matures rapidly toward the late endosome, and a static population that matures much more slowly. Cargos destined for degradation, including low density lipoproteins, epidermal growth factors, and influenza virus, are internalized and targeted to the $Rab5^+$, $EEA1^-$-dynamic population of early endosomes, thereafter trafficking to $Rab7^+$-late endosmes. In contrast, the recycling ligand transferrin is delivered to $Rab5^+$, $EEA1^+$-static early endosomes, followed by translocating to $Rab11^+$-recycling endosomes. Additionally, Burgdorf et al. clearly demonstrated that a mannose receptor introduced OVA specifically into an $EEA\text{-}1^+$, $Rab5^+$-stable early endosomal compartment for subsequent cross-presentation (30). In contrast, pinocytosis conveyed OVA to lysosomes for class II presentation. Of interest, OVA endocytosed by a scavenger receptor did not colocalize with EEA1, but colocalized with LAMP-1 in lysosome, leading to presentation in the context of MHC class II molecules. We showed that the ORP150-peptide complex is targeted into $Rab5^+$, $EEA1^+$-early endosome after internalization by DCs, suggesting that preferential sorting to the static endosome is necessary for cross-presentation of ORP150-peptide complexes. In contrast, soluble OVA protein, which was not cross-presented, targeted to the $EEA1^-$ and $LAMP\text{-}1^+$-dynamic early endosome-late endosome/lysosome pathway, leading to degradation and presentation in the context of MHC class II molecules. These data suggested that ORP150 shuttled the chaperoned precursor peptide into the static endosome-recycling pathway, preventing further degradation, followed by transferring the peptide onto recycling MHC class I molecules. If the ORP150-peptide complexes were loaded into late endosomes/lysosomes, they might be quickly degraded. Therefore, we consider that it is necessary that the ORP150-chaperoned peptide complex targets the early endosome and is processed in the static endosome-recycling pathway.

We have shown that immunization with ORP150-peptide complexes elicits strong CTL responses and antitumor effects. In contrast, we have reported that Hsp70-peptide complex, which is a representative member of Hsp70 superfamily, elicits only weak CTL responses (22). This may be because ORP150 is more efficient in binding peptides than is Hsp70. The ability of ORP150 to bind polypeptides better than other Hsp70 family members is largely due to its enlarged C-terminal helical domain (41, 42). Moreover, it may help that peptide binding to ORP150 is independent of ATP, which is in contrast with ATP-dependent substrate binding of other Hsp70 family members (42).

Finally, to date, SR-A and SREC-I have been identified as receptors for ORP150 expressed on APCs (20). However, whether SR-A or SREC-I is responsible for the efficient cross-presentation by DCs remains unclear. Such receptors should introduce the ORP150-peptide complex specifically into a static early endosomal compartment for the subsequent cross-presentation. Sorting in the endocytic system is a complex and highly dynamic process in which a wide variety of sorting motifs are recognized by specific sorting machinery to direct the membrane protein such as a receptor to its destination. Namely, after the receptor-mediated endocytosis, sorting of the ORP150-Ag complex into the static early endosome may be regulated by specific sorting motifs. The ORP-specific receptor might bear the sorting motifs, which is responsible for the trafficking ORP150 receptor-ORP150 complex to the static early endosomes. To elucidate the mechanism for sorting ORP150 into these compartments, the specific receptors for the ORP150-mediated cross-presentation should be defined. Moreover, it is very important to identify the motifs intrinsic in such receptors that govern static early endosomal sorting. Identification and characterization of the cross-presentation-responsible receptor and its role as an efficient sorter to the static early endosome have important implications in vaccine development strategies. We are currently investigating the ORP150-specific receptors expressed on APCs responsible for the cross-presentation.

Acknowledgments

We thank Dr. N. Shastri for the B3Z and KZO T cell hybridomas.

Disclosures

The authors have no financial conflicts of interest.

References

1. Udono, H., and P. K. Srivastava. 1994. Comparison of tumor-specific immunogenicities of stress-induced proteins gp96, hsp90, and hsp70. *J. Immunol.* 152: 5398–5403.
2. Tamura, Y., P. Peng, K. Liu, M. Daou, and P. K. Srivastava. 1997. Immunotherapy of tumors with autologous tumor-derived heat shock protein preparations. *Science* 278: 117–120.
3. Sato, K., Y. Torimoto, Y. Tamura, M. Shindo, H. Shinzaki, K. Hirai, and Y. Kohgo. 2001. Immunotherapy using heat-shock protein preparations of leukemia cells after syngeneic bone marrow transplantation in mice. *Blood* 98: 1852–1857.
4. Noessner, E., R. Gastpar, V. Milani, A. Brandl, P. J. Hutzler, M. C. Kuppner, M. Roos, E. Kremmer, A. Asea, S. K. Calderwood, and R. D. Issels. 2002. Tumor-derived heat shock protein 70 peptide complexes are cross-presented by human dendritic cells. *J. Immunol.* 169: 5424–5432.
5. Milani, V., E. Noessner, S. Ghose, M. Kuppner, B. Ahrens, A. Scharner, R. Gastpar, and R. D. Issels. 2002. Heat shock protein 70: role in antigen presentation and immune stimulation. *Int. J. Hyperthermia* 18: 563–575.
6. Arnold-Schild, D., D. Hanau, D. Spehner, C. Schmid, H. G. Rammensee, H. de la Salle, and H. Schild. 1999. Cutting edge: receptor-mediated endocytosis of heat shock proteins by professional antigen-presenting cells. *J. Immunol.* 162: 3757–3760.
7. Moroi, Y., M. Mayhew, J. Trcka, M. H. Hoe, Y. Takechi, F. U. Hartl, J. E. Rothman, and A. N. Houghton. 2000. Induction of cellular immunity by immunization with novel hybrid peptides complexed to heat shock protein 70. *Proc. Natl. Acad. Sci. USA* 97: 3485–3490.
8. Singh-Jasuja, H., R. E. Toes, P. Spee, C. Munz, N. Hilf, S. P. Schoenberger, P. Ricciardi-Castagnoli, J. Neefjes, H. G. Rammensee, D. Arnold-Schild, and H. Schild. 2000. Cross-presentation of glycoprotein 96-associated antigens on major histocompatibility complex class I molecules requires receptor-mediated endocytosis. *J. Exp. Med.* 191: 1965–1974.
9. Castelli, C., A. M. Ciupitu, F. Rini, L. Rivoltini, A. Mazzocchi, R. Kiessling, and G. Parmiani. 2001. Human heat shock protein 70 peptide complexes specifically activate antimelanoma T cells. *Cancer Res.* 61: 222–227.
10. Srivastava, P. 2002. Interaction of heat shock proteins with peptides and antigen presenting cells: chaperoning of the innate and adaptive immune responses. *Annu. Rev. Immunol.* 20: 395–425.

11. Ueda, G., Y. Tamura, I. Hirai, K. Kamiguchi, S. Ichimiya, T. Torigoe, H. Hiratsuka, H. Sunakawa, and N. Sato. 2004. Tumor-derived heat shock protein 70-pulsed dendritic cells elicit tumor-specific cytotoxic T lymphocytes (CTLs) and tumor immunity. *Cancer Sci.* 95: 248–253.
12. Asea, A., S. K. Kraeft, E. A. Kurt-Jones, M. A. Stevenson, L. B. Chen, R. W. Finberg, G. C. Koo, and S. K. Calderwood. 2000. HSP70 stimulates cytokine production through a CD14-dependant pathway, demonstrating its dual role as a chaperone and cytokine. *Nat. Med.* 6: 435–442.
13. Asea, A., M. Rehli, E. Kabingu, J. A. Boch, O. Bare, P. E. Auron, M. A. Stevenson, and S. K. Calderwood. 2002. Novel signal transduction pathway utilized by extracellular HSP70: role of Toll-like receptor (TLR) 2 and TLR4. *J. Biol. Chem.* 277: 15028–15034.
14. Binder, R., D. Han, and P. Srivastava. 2000. CD91: a receptor for heat shock protein gp96. *Nat. Immunol.* 1: 151–155.
15. Basu, S., R. J. Binder, T. Ramalingam, and P. K. Srivastava. 2001. CD91 is a common receptor for heat shock proteins gp96, hsp90, hsp70, and calreticulin. *Immunity* 14: 303–313.
16. Binder, R. J., and P. K. Srivastava. 2004. Essential role of CD91 in re-presentation of gp96-chaperoned peptides. *Proc. Natl. Acad. Sci. USA* 101: 6128–6133.
17. Delneste, Y., G. Magistrelli, J. Gauchat, J. Haeuw, J. Aubry, K. Nakamura, N. Kawakami-Honda, L. Goetsch, T. Sawamura, J. Bonnefoy, and P. Jeannin. 2002. Involvement of LOX-1 in dendritic cell-mediated antigen cross-presentation. *Immunity.* 17: 353–362.
18. Becker, T., F. U. Hartl, and F. Wieland. 2002. CD40, an extracellular receptor for binding and uptake of Hsp70-peptide complexes. *J. Cell Biol.* 158: 1277–1285.
19. Berwin, B., J. P. Hart, S. Rice, C. Gass, S. V. Pizzo, S. R. Post, and C. V. Nicchitta. 2003. Scavenger receptor-A mediates gp96/GRP94 and calreticulin internalization by antigen-presenting cells. *EMBO J.* 22: 6127–6136.
20. Facciponte, J. G., X. Y. Wang, and J. R. Subjeck. 2007. Hsp110 and Grp170, members of the Hsp70 superfamily, bind to scavenger receptor-A and scavenger receptor expressed by endothelial cells-I. *Eur. J. Immunol.* 37: 2268–2279.
21. Berwin, B., Y. Delneste, R. V. Lovingood, S. R. Post, and S. V. Pizzo. 2004. SREC-I, a type F scavenger receptor, is an endocytic receptor for calreticulin. *J. Biol. Chem.* 279: 51250–51257.
22. Kurotaki, T., Y. Tamura, G. Ueda, J. Oura, G. Kutomi, Y. Hirohashi, H. Sahara, T. Torigoe, H. Hiratsuka, H. Sunakawa, et al. 2007. Efficient cross-presentation by heat shock protein 90-peptide complex-loaded dendritic cells via an endosomal pathway. *J. Immunol.* 179: 1803–1813.
23. Kuwabara, K., M. Matsumoto, J. Ikeda, O. Hori, S. Ogawa, Y. Maeda, K. Kitagawa, N. Imuta, T. Kinoshita, D. M. Stern, et al. 1996. Purification and characterization of a novel stress protein, the 150-kDa oxygen-regulated protein (ORP150), from cultured rat astrocytes and its expression in ischemic mouse brain. *J. Biol. Chem.* 271: 5025–5032.
24. Ikeda, J., S. Kaneda, K. Kuwabara, S. Ogawa, T. Kobayashi, M. Matsumoto, T. Yura, and H. Yanagi. 1997. Cloning and expression of cDNA encoding the human 150 kDa oxygen-regulated protein, ORP150. *Biochem. Biophys. Res. Commun.* 230: 94–99.
25. Wang, X. Y., L. Kazim, E. A. Repasky, and J. R. Subjeck. 2001. Characterization of heat shock protein 110 and glucose-regulated protein 170 as cancer vaccines and the effect of fever-range hyperthermia on vaccine activity. *J. Immunol.* 166: 490–497.
26. Wang, X. Y., L. Kazim, E. A. Repasky, and J. R. Subjeck. 2003. Immunization with tumor-derived ER chaperone grp170 elicits tumor-specific $CD8^+$ T-cell responses and reduces pulmonary metastatic disease. *Int. J. Cancer* 105: 226–231.
27. Wang, X. Y., H. Arnouk, X. Chen, L. Kazim, E. A. Repasky, and J. R. Subjeck. 2006. Extracellular targeting of endoplasmic reticulum chaperone glucose-regulated protein 170 enhances tumor immunity to a poorly immunogenic melanoma. *J. Immunol.* 177: 1543–1551.
28. Park, J. E., J. Facciponte, X. Chen, I. MacDonald, E. A. Repasky, M. H. Manjili, X. Y. Wang, and J. R. Subjeck. 2006. Chaperoning function of stress protein grp170, a member of the hsp70 superfamily, is responsible for its immunoadjuvant activity. *Cancer Res.* 66: 1161–1168.
29. Lakadamyali, M., M. J. Rust, and X. Zhuang. 2006. Ligands for clathrin-mediated endocytosis are differentially sorted into distinct populations of early endosomes. *Cell* 124: 997–1009.
30. Burgdorf, S., A. Kautz, V. Bohnert, P. A. Knolle, and C. Kurts. 2007. Distinct pathways of antigen uptake and intracellular routing in CD4 and CD8 T cell activation. *Science* 316: 612–616.
31. Gotoh, M., H. Takasu, K. Harada, and T. Yamaoka. 2002. Development of HLA-A2402/K^b transgenic mice. *Int. J. Cancer* 100: 565–570.
32. Hirohashi, Y., T. Torigoe, A. Maeda, Y. Nabeta, K. Kamiguchi, T. Sato, J. Yoda, H. Ikeda, K. Hirata, N. Yamanaka, and N. Sato. 2002. An HLA-A24-restricted cytotoxic T lymphocyte epitope of a tumor-associated protein, survivin. *Clin. Cancer Res.* 8: 1731–1739.
33. Tsuruma, T., Y. Iwayama, T. Ohmura, T. Katsuramaki, F. Hata, T. Furuhata, K. Yamaguchi, Y. Kimura, T. Torigoe, N. Toyota, et al. 2008. Clinical and immunological evaluation of anti-apoptosis protein, survivin-derived peptide vaccine in phase I clinical study for patients with advanced or recurrent breast cancer. *J. Transl. Med.* 6: 24.
34. Ramirez, S. R., H. Singh-Jasuja, T. Warger, S. Braedel-Ruoff, N. Hilf, K. Wiemann, H. G. Rammensee, and H. Schild. 2005. Glycoprotein 96-activated dendritic cells induce a CD8-biased T cell response. *Cell Stress Chaperones* 10: 221–229.
35. Bendz, H., S. C. Ruhland, M. J. Pandya, O. Hainzl, S. Riegelsberger, C. Brauchle, M. P. Mayer, J. Buchner, R. D. Issels, and E. Noessner. 2007. Human heat shock protein 70 enhances tumor antigen presentation through complex formation and intracellular antigen delivery without innate immune signaling. *J. Biol. Chem.* 282: 31688–31702.
36. Doody, A. D., J. T. Kovalchin, M. A. Mihalyo, A. T. Hagymasi, C. G. Drake, and A. J. Adler. 2004. Glycoprotein 96 can chaperone both MHC class I- and class II-restricted epitopes for in vivo presentation, but selectively primes $CD8^+$ T cell effector function. *J. Immunol.* 172: 6087–6092.
37. SenGupta, D., P. J. Norris, T. J. Suscovich, M. Hassan-Zahraee, H. F. Moffett, A. Trocha, R. Draenert, P. J. Goulder, R. J. Binder, D. L. Levey, et al. 2004. Heat shock protein-mediated cross-presentation of exogenous HIV antigen on HLA class I and class II. *J. Immunol.* 173: 1987–1993.
38. Asea, A. 2005. Stress proteins and initiation of immune response: chaperokine activity of hsp72. *Exerc. Immunol. Rev.* 11: 34–45.
39. Suto, R., and P. K. Srivastava. 1995. A mechanism for the specific immunogenicity of heat shock protein-chaperoned peptides. *Science* 269: 1585–1588.
40. Kleijmeer, M. J., J. M. Escola, F. G. UytdeHaag, E. Jakobson, J. M. Griffith, A. D. Osterhaus, W. Stoorvogel, C. J. Melief, C. Rabouille, and H. J. Geuze. 2001. Antigen loading of MHC class I molecules in the endocytic tract. *Traffic* 2: 124–137.
41. Dierks, T., J. Volkmer, G. Schlenstedt, C. Jung, U. Sandholzer, K. Zachmann, P. Schlotterhose, K. Neifer, B. Schmidt, and R. Zimmermann. 1996. A microsomal ATP-binding protein involved in efficient protein transport into the mammalian endoplasmic reticulum. *EMBO J.* 15: 6931–6942.
42. Spee, P., J. Subjeck, and J. Neefjes. 1999. Identification of novel peptide binding proteins in the endoplasmic reticulum: ERp72, calnexin, and grp170. *Biochemistry* 38: 10559–10566.

Int. J. Hyperthermia, December 2009; 25(8): 610–616

informa
healthcare

RESEARCH ARTICLE

Heat shock proteins and immunity: Application of hyperthermia for immunomodulation

TOSHIHIKO TORIGOE, YASUAKI TAMURA, & NORIYUKI SATO

Department of Pathology, Sapporo Medical University School of Medicine, Sapporo, Japan

(Received 21 March 2009; Revised 1 September 2009; Accepted 7 September 2009)

Abstract
Heat shock proteins (HSPs) play an important role as 'endogenous danger signals' in the immune surveillance system. Extracellular HSPs released from damaged cells can stimulate professional antigen-presenting cells, followed by cytokine release and expression of cell surface molecules. In addition to such activity stimulating innate immunity, extracellular HSPs can promote the cross-presentation of HSP-bound peptide antigens to MHC class I molecules in dendritic cells, leading to efficient induction of antigen-specific cytotoxic T-lymphocytes. The roles of HSPs stimulating both innate immunity and adaptive immunity can explain at least in part the molecular mechanism by which thermal stress bolsters the host immune system. In the present review, we present novel aspects of the roles of HSPs in immunity and discuss the therapeutic application of hyperthermia for immunomodulation.

Keywords: *heat shock and immune response, immunotherapy, MHC class I, dendritic cells, antigen presentation*

The role of intracellular HSPs in antigen processing and presentation

Heat shock proteins (HSPs) act as molecular chaperones inside cells, regulating conformational change, translocation, assembly and degradation of cellular proteins. They have important roles in cellular protection against various stresses such as ischaemia, heat stress and oxidative stress [1–3]. They are also involved in the antigen processing and presentation machinery as chaperones for antigenic proteins and peptides. A number of studies have shown that the 70 kDa HSP family (Hsp70) and 90 kDa HSP family (Hsp90) are associated with antigenic peptides in the cytosol and mediate their translocation and processing [4]. We have demonstrated previously that Hsp70 is associated with transporters associated with antigen processing (TAP) and mediates ATP-dependent transportation of antigenic peptides from cytosol to endoplasmic reticulum (ER) [5]. The efficiency of the transportation is correlated with affinity of the peptides to Hsp70, indicating that HSPs might serve as intracellular antigen transporters. HSPs are also associated with proteasomes, which degrade cellular proteins and produce antigenic peptides [6] (Figure 1). In virus-infected cells, viral proteins bind to HSPs to utilise the protein folding machinery. However, some HSP-bound viral proteins are degraded by proteasomes and presented to MHC class I, leading to recognition of the infected cells by cytotoxic T-lymphocytes (CTL). Therefore, increased body temperature and the subsequent HSP induction are important reactions in the host defence system.

The role of extracellular HSPs in innate immune responses

Pattern recognition molecules have crucial roles in innate immune responses. So far, a number of Toll-like receptor (TLR) ligands have been reported, including lipopolysaccharides, peptidoglycans, CpG oligodeoxynucleotides and double-stranded RNA [7].

Correspondence: Toshihiko Torigoe, MD, PhD, Department of Pathology, Sapporo Medical University School of Medicine, 060-8556 Sapporo, Japan. Tel: +81-11-613-8374. Fax: +81-11-643-2310. E-mail: torigoe@sapmed.ac.jp

ISSN 0265-6736 print/ISSN 1464–5157 online
DOI: 10.3109/02656730903315831

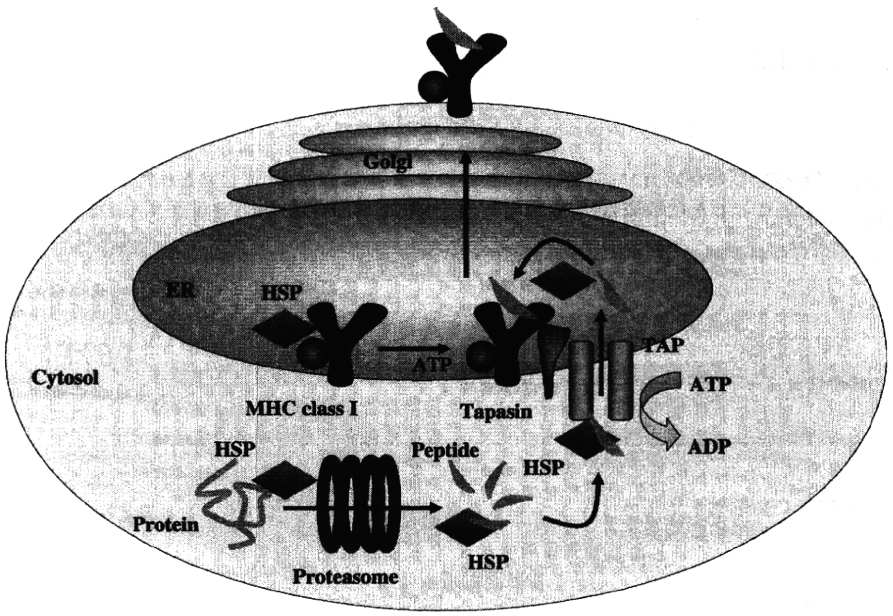

Figure 1. The role of intracellular HSPs in MHC class I antigen presentation. Cellular proteins are degraded by proteasomes, resulting in production of antigenic peptides. The peptides are transported from the cytosol into the endoplasmic reticulum (ER) by transporters associated with antigen processing (TAP), followed by binding to MHC class I molecules and presentation on the cell surface. Molecular chaperone HSPs are associated with antigenic peptides, proteasomes, TAP and MHC class I in this pathway.

In addition to the TLR ligands derived from microorganisms, silica crystals, aluminum salt and asbestos are known to stimulate NOD family molecules [8–11]. It is well known that most of these exogenous foreign molecules activate dendritic cells (DCs) and induce release of cytokines, including TNF-α, interferon and IL-12. Recently, it was revealed that extracellular HSPs could activate DCs as well as exogenous TLR ligands [12, 13]. Hsp70 and Hsp60 are reported to stimulate DCs through TLR4. We have reported that stimulation of DCs with purified Hsp70 results in induction of TNF-α release in a dose-dependent manner, which is inhibited in the presence of Hsp70-targeting polyamine compound deoxyspergualin [14]. Though it has been argued that the pro-inflammatory effects of extracellular HSPs might be mediated through contamination of LPS or other microbial compounds [15], it is true that some aspects of TLR activation by HSPs differ from TLR activation by microbial compounds. For example, activation of TLR signalling by Hsp60 requires endocytosis, whereas that by LPS does not [16]. In another study, it was shown that Hsp70 triggered calcium-mediated signalling in DCs, whereas it was not observed in LPS-triggering signals through TLR [17]. In order to ensure that LPS contamination with Hsp70 was not responsible for the release of cytokines, Hsp70 was either boiled at 95 °C or treated with proteinase K; however, both of these treatments abrogated Hsp70-induced, but not LPS-induced, release of cytokines, providing further evidence against endotoxin contamination contributing to DC activation [17]. Therefore, HSPs are now recognised as 'endogenous danger signals' that can alert the innate immune system in response to cellular damage. The molecular chaperone Hsp70, with cytokine-like activity in relation to DCs, was termed a 'chaperokine' [18]. HSPs released from damaged cells can activate DCs at the site of the injury and induce inflammatory cytokine release (Figure 2). Since the magnitude of the innate immune response is correlated with the amount of extracellular HSPs, more damaged cells and more severe stress can elicit more robust immune responses [14]. Therefore, local hyperthermia treatment might enhance the innate immune response through induction of a heat shock response and extracellular release of HSPs [13].

The role of extracellular HSPs in adaptive immunity

It has been shown that Hsp70 and Gp96, a member of the Hsp90 family, extracted from tumour cells can elicit anti-tumour CTL responses after vaccination in mouse models [19]. The immunogenic tumour antigens recognised by the CTLs are not HSPs themselves, but HSP-bound proteins and peptides [20]. Since HSPs are associated with

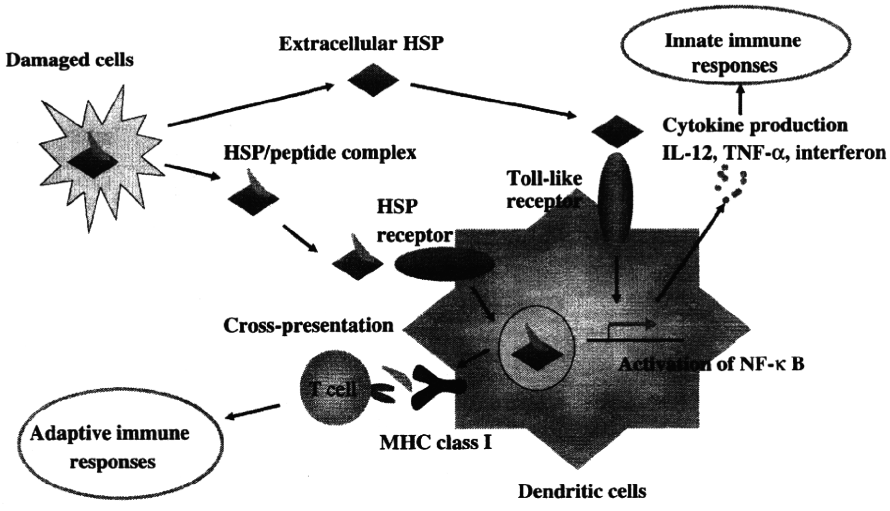

Figure 2. The role of extracellular HSPs in immune responses. Extracellular HSPs can stimulate Toll-like receptors, leading to activation of dendritic cells and release of cytokines such as IL-12, TNF-α and interferon (innate immune responses). Extracellular HSPs can be internalised through HSP receptors with HSP-bound peptides. The antigenic peptides are then cross-presented to MHC class I molecules, leading to induction of peptide-specific CTL responses (adaptive immune responses).

many cellular proteins, especially denatured proteins or mutated proteins in tumour cells, the antigenic proteins can be taken into professional APC in association with HSPs and presented to MHC class I molecules, leading to antigen-specific CTL induction [21, 22]. MHC class I presents peptides derived from endogenous proteins in non-APC. On the other hand, MHC class I can present peptides derived from exogenous proteins in professional APC as well, which is termed 'cross-presentation'. Extracellular HSPs were suggested to enhance cross-presentation of HSP-bound antigens to MHC class I in DCs. However, it remained unclear for a long time how HSPs could facilitate the cross-presentation and induction of CTLs. In 2000 it was reported that a Gp96-peptide complex could be taken into DCs via receptor-mediated endocytosis, and the receptor for Gp96 was CD91, an alpha2-macroglobulin receptor [23]. Basu et al. showed that not only Gp96, but also Hsp90, Hsp70 and calreticulin used CD91 as a common receptor [24]. Following the initial reports, other molecules were shown to be receptors for Hsp70 and Gp96, including CD40 [25] and the scavenger receptor family members LOX-1 [26] and SR-A [27]. Thus, it became evident that DCs could internalise HSP-chaperoned proteins and peptides through various receptors by endocytosis [28, 29]. We have analysed the antigen-processing pathway for cross-presentation after endocytosis. We showed that internalised Hsp70 or Hsp90 was transported preferentially into the early endosome and not to the ER or lysosome in DCs [30]. HSP-bound antigens are then processed in the endosome, followed by presentation through recycling MHC class I molecules (endosomal pathway), or translocated into the cytosol, followed by processing through proteasome-TAP machinery and presentation through MHC class I in the ER (TAP-ER pathway) [31–38] (Figure 3). It is proposed that DCs may have a unique membrane-transport pathway linking the endosomal compartment to the cytosolic compartment [39].

In addition, we have found that HSPs, especially Hsp90, have a potent endosome-targeting capability in professional APCs [38, 40]. Hsp90-chaperoned proteins were presented much more selectively through the MHC class I pathway (early endosomal pathway) than through the MHC class II pathway (late endosomal pathway). In contrast, free proteins are presented preferentially through the MHC class II pathway but not through the MHC class I pathway, resulting in antibody responses rather than CTL responses.

These studies clarified novel roles of extracellular HSPs in adaptive immunity. Professional APCs can present extracellular HSP-bound peptides/proteins to MHC class I and induce antigen-specific CTL responses. The HSP-mediated cross-presentation is more rapid and efficient than free antigens, indicating that extracellular HSPs can activate not only innate immune responses but also adaptive immune responses.

Application of HSPs for vaccine development

On the basis of the immunostimulatory activity of HSPs, we examined the application of HSPs for

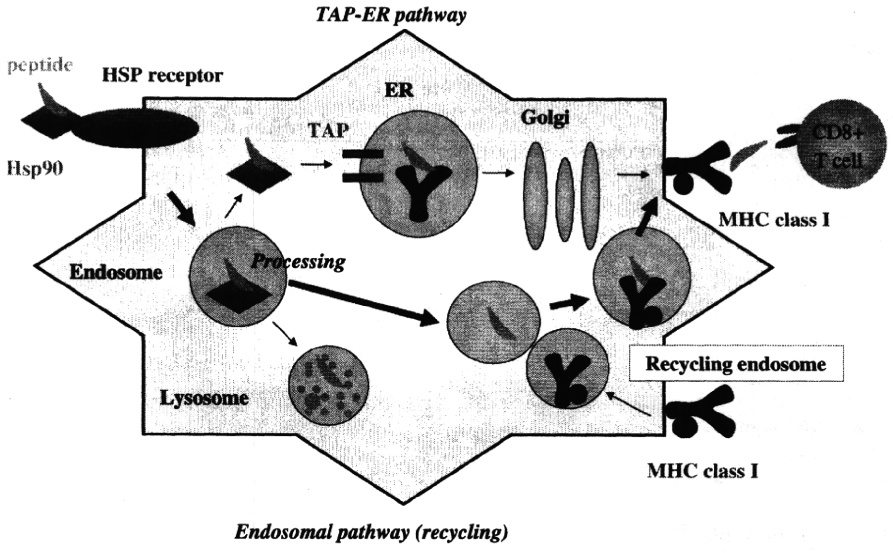

Figure 3. Cross-presentation pathway of Hsp90-antigen complex. HSP-antigen complexes internalised through HSP receptors are transported into the early endosome, followed by processing and presentation through MHC class I in the recycling endosome. Some of the HSP-antigen complexes may be released into the cytosol, followed by transportation through TAP and presentation through MHC class I in the ER.

vaccine adjuvant. Activation of DCs is required to achieve an efficient immune response to vaccination. Thus far, some TLR ligands such as CpG oligodeoxynucleotides and peptidoglycans have been employed as adjuvants as well as classical Freund adjuvants. However, most of the trials failed due to severe adverse effects or lack of effectiveness. The safe and common adjuvants in clinical use at present are mineral oil (Freund incomplete adjuvant) and aluminium. In animal models we compared the efficiency of peptide-specific CTL induction among peptide vaccines with various compositions such as peptide + PBS, peptide + Freund adjuvant, peptide + CpG oligodeoxynucleotide, peptide + Hsp70 and peptide + Hsp90 [38]. It was demonstrated that efficient CTL induction was achieved via vaccination with peptide + Hsp90 or peptide + complete Freund adjuvant (CFA) (Figure 4). However, vaccination with peptide + CFA caused severe local inflammation with skin ulceration. In contrast, there was no obvious side effect in the case of Hsp90 vaccination, indicating the superior safety and immunostimulatory action of Hsp90. Successful immunisation was also demonstrated in a mouse tumour therapeutic model. Vaccination of tumour-bearing mice with peptide + Hsp90 resulted in tumour regression and increased survival [38]. The results represent the greater advantage of utilising 'endogenous danger signals' in the development of vaccine as compared to 'exogenous danger signals', which are less physiological. Our study provides a rationale for a novel vaccine strategy in the field of cancer and infective diseases.

Application of hyperthermia for immunomodulation

It has been reported that hyperthermia in the febrile range could induce heat shock responses and subsequent HSP expression in human cells [41]. Therefore, the roles of intracellular and extracellular HSPs in the immune system can explain at least in part the benefits of fever in infectious diseases [42]. In addition to the HSP-family genes, expression of a number of immunomodulatory genes are induced during febrile-range hyperthermia, including cell adhesion molecules such as ICAM-1/CD54, JAM3, CD11b and CD47, TLRs such as TLR-6 and TLR-7, chemokines such as CXCL-5, CXCL-7 and IL-8, and prostaglandin E synthase [43]. There is accumulating evidence that fever-range thermal stress bolsters primary immune surveillance of lymphoid organs by augmenting lymphocyte extravasation across specialised blood vessels termed high endothelial venules (HEVs) [44–47]. Chen et al. showed that thermal stress enhanced endothelial expression of ICAM-1/CD54 and CCL21 chemokine, leading to increased lymphocyte trafficking across HEVs [48–50]. These mechanisms substantially increase the probability of antigen-specific T cells encountering the APCs in lymphoid organs. They also revealed that one of the important mediators of thermal effects upon lymphocytes and HEVs was IL-6 trans-signalling [48, 49]. These data suggest that hyperthermia treatment that is clinically applied as adjuvant treatment for sarcoma, melanoma and cervical cancer might be effective in the

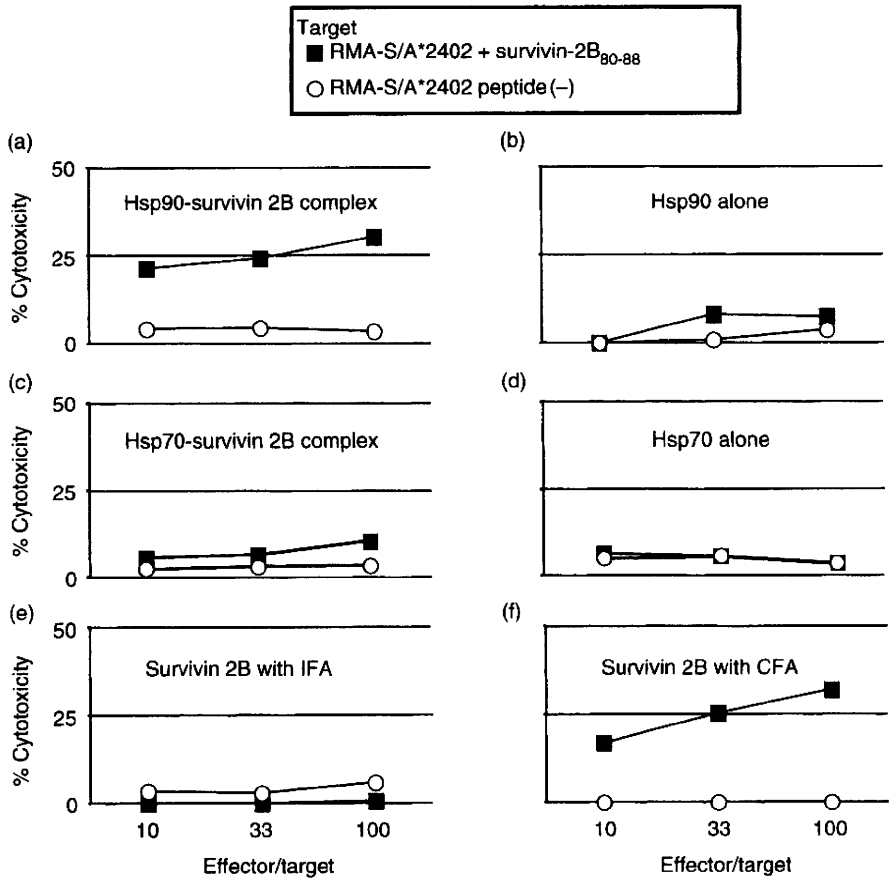

Figure 4. Hsp90-peptide vaccine can induce an efficient specific CTL response. HLA-A*2402/Kb-transgenic mice were immunised four times with the indicated peptide vaccination. Spleen cells were removed one week after the last immunisation, cultured for five days with survivin-2B80–88 peptides, and tested for cytotoxicity. Each line represents the specific lysis of target cells by spleen cells from one individual mouse. Target cells were RMA-S/A*2402 cells pulsed with the survivin-2B80–88 peptide, or without the peptide. Note that CTL were induced in the cases of vaccination with Hsp90 + peptide and complete Freund adjuvant (CFA) + peptide. IFA: incomplete Freund adjuvant. (Figure from reference [38]). Copyright 2007. The American Association of Immunologists, Inc.

enhancement of anti-tumour immune responses [51–53]. CTL-inducible HSP vaccine immunotherapy might be developed in combination with hyperthermia. However, the optimum temperature and duration of hyperthermia for the purpose of immunomodulation remain unclear and have to be determined through further studies, since they are quite distinct from the cytotoxic conditions utilised in the field of cancer therapy. Thermal effects on the immune responses can be achieved in the fever-range temperature (38–41 °C) [48], whereas cytotoxic effects of thermal stress can be achieved in the non-physiological range temperature (over 42 °C). In addition, it has been reported that thermal stress in certain condition can suppress the innate immune responses in macrophages [54, 55].

It is expected that hyperthermia and HSP vaccine might be applicable to the treatment of autoimmune diseases such as type I diabetes and rheumatoid arthritis [56]. The rationale came from the evidence that self-HSP-specific CD4-positive T-cells have been found in association with chronic inflammatory diseases and the HSP-specific T-cells have an immunoregulatory phenotype that can suppress immune responses in autoimmune diseases [56–58]. Indeed, there have been some clinical trials of HSP vaccine for the treatment of rheumatoid arthritis and type I diabetes [59, 60]. There is a report of an animal model showing that whole-body hyperthermia could attenuate autoimmune myocarditis [61]. It is suggested that hyperthermia-mediated induction of endogenous HSPs might facilitate the induction of CD4-positive immunoregulatory T-cells. As we discussed above, Hsp90-bound antigenic peptides could elicit strong peptide-specific CD8-positive cytotoxic T-cell responses through the stimulation of DCs. However, Hsp60 and Hsp70 could induce CD4-positive regulatory T-cell responses in certain conditions [56]. It seems that the direction of HSP-mediated immune response differs among different HSP family proteins and different HSP-bound antigens. Therefore, it is possible that hyperthermia

treatment causes a distinct effect on the immune response, either immunogenic or tolerogenic, depending on the tissue and the temperature. Though further studies will be required to develop a novel therapeutic strategy, there are promising advances in the fields of thermal medicine and immunotherapy.

Declaration of interest: The authors report no conflicts of interest. The authors alone are responsible for the content and writing of the paper.

References

1. Franklin TB, Krueger-Naug AM, Clarke DB, Arrigo AP, Currie RW. The role of heat shock proteins Hsp70 and Hsp27 in cellular protection of the central nervous system. Int J Hyperthermia 2005;21:379–392.
2. Latchman DS. HSP27 and cell survival in neurones. Int J Hyperthermia 2005;21:393–402.
3. Lanneau D, Brunet M, Frisan E, Solary E, Fontenay M, Garrido C. Heat shock proteins: Essential proteins for apoptosis regulation. J Cell Mol Med 2008;12:743-761.
4. Ishii T, Udono H, Yamano T, Ohta H, Uenaka A, Ono T, Hizuta A, Tanaka N, Srivastava PK, Nakayama E. Isolation of MHC class I-restricted tumor antigen peptide and its precursors associated with heat shock proteins hsp70, hsp90, and gp96. J Immunol 1999;162:1303–1309.
5. Kamiguchi K, Torigoe T, Fujiwara O, Ohshima S, Hirohashi Y, Sahara H, Hirai I, Kohgo Y, Sato N. Disruption of the association of 73 kDa heat shock cognate protein with transporters associated with antigen processing (TAP) decreases TAP-dependent translocation of antigenic peptides into the endoplasmic reticulum. Microbiol Immunol 2008;52:94–106.
6. Yamano T, Murata S, Shimbara N, Tanaka N, Chiba T, Tanaka K, Yui K, Udono H. Two distinct pathways mediated by PA28 and hsp90 in major histocompatibility complex class I antigen processing. J Exp Med 2002;196:185–196.
7. Jin MS, Lee JO. Structures of the toll-like receptor family and its ligand complexes. Immunity 2008;29:182–191.
8. Martinon F, Gaide O, Petrilli V, Mayor A, Tschopp J. NALP inflammasomes: A central role in innate immunity. Semin Immunopathol 2007;29:213–229.
9. Dostert C, Petrilli V, Van Bruggen R, Steele C, Mossman BT, Tschopp J. Innate immune activation through Nalp3 inflammasome sensing of asbestos and silica. Science 2008;320:674–677.
10. Eisenbarth SC, Colegio OR, O'Connor W, Sutterwala FS, Flavell RA. Crucial role for the Nalp3 inflammasome in the immunostimulatory properties of aluminium adjuvants. Nature 2008;453:1122–1126.
11. Hornung V, Bauernfeind F, Halle A, Samstad EO, Kono H, Rock KL, Fitzgerald KA, Latz E. Silica crystals and aluminum salts activate the NALP3 inflammasome through phagosomal destabilization. Nat Immunol 2008;9:847–856.
12. Asea A, Rehli M, Kabingu E, Boch JA, Bare O, Auron PE, Stevenson MA, Calderwood SK. Novel signal transduction pathway utilized by extracellular HSP70: Role of toll-like receptor (TLR) 2 and TLR4. J Biol Chem 2002;277: 15028–15034.
13. Chen T, Guo J, Han C, Yang M, Cao X. Heat shock protein 70, released from heat-stressed tumor cells, initiates antitumor immunity by inducing tumor cell chemokine production and activating dendritic cells via TLR4 pathway. J Immunol 2009;182:1449–1459.
14. Sugawara A, Torigoe T, Tamura Y, Kamiguchi K, Nemoto K, Oguro H, Sato N. Polyamine compound deoxyspergualin inhibits heat shock protein-induced activation of immature dendritic cells. Cell Stress Chaperones 2009;14:133–139.
15. Bausinger H, Lipsker D, Ziylan U, Manie S, Briand JP, Cazenave JP, Muller S, Haeuw JF, Ravanat C, de la Salle H, Hanau D. Endotoxin-free heat-shock protein 70 fails to induce APC activation. Eur J Immunol 2002;32:3708–3713.
16. Vabulas RM, Ahmad-Nejad P, da Costa C, Miethke T, Kirschning CJ, Hacker H, Wagner H. Endocytosed HSP60s use toll-like receptor 2 (TLR2) and TLR4 to activate the toll/interleukin-1 receptor signaling pathway in innate immune cells. J Biol Chem 2001;276:31332–31339.
17. MacAry PA, Javid B, Floto RA, Smith KG, Oehlmann W, Singh M, Lehner PJ. HSP70 peptide binding mutants separate antigen delivery from dendritic cell stimulation. Immunity 2004;20:95–106.
18. Asea A. Hsp70: A chaperokine. Novartis Found Symp;291:173–9; discussion 9-83, 221-4, 2008.
19. Srivastava PK, Old LJ. Identification of a human homologue of the murine tumor rejection antigen GP96. Cancer Res 1989;49:1341–1343.
20. Srivastava PK, Udono H, Blachere NE, Li Z. Heat shock proteins transfer peptides during antigen processing and CTL priming. Immunogenetics 1994;39:93–98.
21. Udono H, Levey DL, Srivastava PK. Cellular requirements for tumor-specific immunity elicited by heat shock proteins: Tumor rejection antigen gp96 primes CD8+ T cells in vivo. Proc Natl Acad Sci USA 1994;91:3077–3081.
22. Tamura Y, Peng P, Liu K, Daou M, Srivastava PK. Immunotherapy of tumors with autologous tumor-derived heat shock protein preparations. Science 1997;278:117–120.
23. Binder RJ, Han DK, Srivastava PK. CD91: A receptor for heat shock protein gp96. Nat Immunol 2000;1:151–155.
24. Basu S, Binder RJ, Ramalingam T, Srivastava PK. CD91 is a common receptor for heat shock proteins gp96, hsp90, hsp70, and calreticulin. Immunity 2001;14:303–313.
25. Becker T, Hartl FU, Wieland F. CD40, an extracellular receptor for binding and uptake of Hsp70-peptide complexes. J Cell Biol 2002;158:1277–1285.
26. Delneste Y, Magistrelli G, Gauchat J, Haeuw J, Aubry J, Nakamura K, Kawakami-Honda N, Goetsch L, Sawamura T, Bonnefoy J, Jeannin P. Involvement of LOX-1 in dendritic cell-mediated antigen cross-presentation. Immunity 2002;17:353–362.
27. Berwin B, Hart JP, Rice S, Gass C, Pizzo SV, Post SR, Nicchitta CV. Scavenger receptor-A mediates gp96/GRP94 and calreticulin internalization by antigen-presenting cells. Embo J 2003;22:6127–6136.
28. Binder RJ, Srivastava PK. Essential role of CD91 in re-presentation of gp96-chaperoned peptides. Proc Natl Acad Sci USA 2004;101:6128–6133.
29. Delneste Y. Scavenger receptors and heat-shock protein-mediated antigen cross-presentation. Biochem Soc Trans 2004;32:633–635.
30. Ueda G, Tamura Y, Hirai I, Kamiguchi K, Ichimiya S, Torigoe T, Hiratsuka H, Sunakawa H, Sato N. Tumor-derived heat shock protein 70-pulsed dendritic cells elicit tumor-specific cytotoxic T lymphocytes (CTLs) and tumor immunity. Cancer Sci 2004;95:248–253.
31. Noessner E, Gastpar R, Milani V, Brandl A, Hutzler PJ, Kuppner MC, Roos M, Kremmer E, Asea A, Calderwood SK, et al. Tumor-derived heat shock protein 70 peptide complexes are cross-presented by human dendritic cells. J Immunol 2002;169:5424–5432.

32. Milani V, Noessner E, Ghose S, Kuppner M, Ahrens B, Scharner A, Gastpar R, Issels RD. Heat shock protein 70: Role in antigen presentation and immune stimulation. Int J Hyperthermia 2002;18:563–575.
33. Bendz H, Ruhland SC, Pandya MJ, Hainzl O, Riegelsberger S, Brauchle C, Mayer MP, Buchner J, Issels RD, Noessner E. Human heat shock protein 70 enhances tumor antigen presentation through complex formation and intracellular antigen delivery without innate immune signaling. J Biol Chem 2007;282:31688–31702.
34. Tobian AA, Canaday DH, Boom WH, Harding CV. Bacterial heat shock proteins promote CD91-dependent class I MHC cross-presentation of chaperoned peptide to CD8+ T cells by cytosolic mechanisms in dendritic cells versus vacuolar mechanisms in macrophages. J Immunol 2004;172:5277–5286.
35. Tobian AA, Canaday DH, Harding CV. Bacterial heat shock proteins enhance class II MHC antigen processing and presentation of chaperoned peptides to CD4+ T cells. J Immunol 2004;173:5130–5137.
36. Tobian AA, Harding CV, Canaday DH. Mycobacterium tuberculosis heat shock fusion protein enhances class I MHC cross-processing and -presentation by B lymphocytes. J Immunol 2005;174:5209–5214.
37. Enomoto Y, Bharti A, Khaleque AA, Song B, Liu C, Apostolopoulos V, Xing PX, Calderwood SK, Gong J. Enhanced immunogenicity of heat shock protein 70 peptide complexes from dendritic cell-tumor fusion cells. J Immunol 2006;177:5946–5955.
38. Kurotaki T, Tamura Y, Ueda G, Oura J, Kutomi G, Hirohashi Y, Sahara H, Torigoe T, Hiratsuka H, Sunakawa H, et al. Efficient cross-presentation by heat shock protein 90-peptide complex-loaded dendritic cells via an endosomal pathway. J Immunol 2007;179:1803–1813.
39. Rodriguez A, Regnault A, Kleijmeer M, Ricciardi-Castagnoli P, Amigorena S. Selective transport of internalized antigens to the cytosol for MHC class I presentation in dendritic cells. Nat Cell Biol 1999;1:362–368.
40. Kutomi G, Tamura Y, Okuya, K, Torigoe T, Sato N. Targeting to static endosome is required for efficient cross-presentation of ER-resident oxygen regulated protein 150 (ORP150)-peptide complexes. J Immunol 2009; in press.
41. Tulapurkar ME, Asiegbu BE, Singh IS, Hasday JD. Hyperthermia in the febrile range induces HSP72 expression proportional to exposure temperature but not to HSF-1 DNA-binding activity in human lung epithelial A549 cells. Cell Stress Chaperones 2009.
42. Hasday JD, Fairchild KD, Shanholtz C. The role of fever in the infected host. Microbes Infect 2000;2:1891–1904.
43. Sonna LA, Hawkins L, Lissauer ME, Maldeis P, Towns M, Johnson SB, Moore R, Singh I, Cowan S, Hasday MJ, JD. Core temperature correlates with expression of selected stress and immunomodulatory genes in febrile patients with sepsis and noninfectious SIRS. Cell Stress Chaperones 2009.
44. Wang WC, Goldman LM, Schleider DM, Appenheimer MM, Subjeck JR, Repasky EA, Evans SS. Fever-range hyperthermia enhances L-selectin-dependent adhesion of lymphocytes to vascular endothelium. J Immunol 1998;160:961–969.
45. Evans SS, Bain MD, Wang WC. Fever-range hyperthermia stimulates alpha4beta7 integrin-dependent lymphocyte-endothelial adhesion. Int J Hyperthermia 2000;16:45–59.
46. Evans SS, Wang WC, Bain MD, Burd R, Ostberg JR, Repasky EA. Fever-range hyperthermia dynamically regulates lymphocyte delivery to high endothelial venules. Blood 2001;97: 2727–2733.
47. Shah A, Unger E, Bain MD, Bruce R, Bodkin J, Ginnetti J, Wang WC, Seon B, Stewart CC, Evans SS. Cytokine and adhesion molecule expression in primary human endothelial cells stimulated with fever-range hyperthermia. Int J Hyperthermia 2002;18:534–551.
48. Chen Q, Fisher DT, Clancy KA, Gauguet JM, Wang WC, Unger E, Rose-John S, von Andrian UH, Baumann H, Evans SS. Fever-range thermal stress promotes lymphocyte trafficking across high endothelial venules via an interleukin 6 trans-signaling mechanism. Nat Immunol 2006;7:1299–1308.
49. Evans SS, Fisher DT, Skitzki JJ, Chen Q. Targeted regulation of a lymphocyte-endothelial-interleukin-6 axis by thermal stress. Int J Hyperthermia 2008;24:67–78.
50. Chen Q, Appenheimer MM, Muhitch JB, Fisher DT, Clancy KA, Miecznikowski JC, Wang WC, Evans SS. Thermal facilitation of lymphocyte trafficking involves temporal induction of intravascular ICAM-1. Microcirculation 2009;16: 143–158.
51. Overgaard J, Gonzalez Gonzalez D, Hulshof MC, Arcangeli G, Dahl O, Mella O, Bentzen SM. Hyperthermia as an adjuvant to radiation therapy of recurrent or metastatic malignant melanoma. A multicentre randomized trial by the European Society for Hyperthermic Oncology. 1996. Int J Hyperthermia 2009;25:323–334.
52. Pennacchioli E, Fiore M, Gronchi A. Hyperthermia as an adjunctive treatment for soft-tissue sarcoma. Expert Rev Anticancer Ther 2009;9:199–210.
53. Franckena M, Fatehi D, de Bruijne M, Canters RA, van Norden Y, Mens JW, van Rhoon GC, van der Zee J. Hyperthermia dose-effect relationship in 420 patients with cervical cancer treated with combined radiotherapy and hyperthermia. Eur J Cancer 2009;45:1969–1978.
54. Singh I, Viscardi S, Kalvakolanu RM, Calderwood I, Hasday S, JD. Inhibition of tumor necrosis factor-alpha transcription in macrophages exposed to febrile range temperature. A possible role for heat shock factor-1 as a negative transcriptional regulator. J Biol Chem 2000;275:9841–9848.
55. Singh IS, He JR, Calderwood S, Hasday JD. A high affinity HSF-1 binding site in the 5′-untranslated region of the murine tumor necrosis factor-alpha gene is a transcriptional repressor. J Biol Chem 2002;277:4981–4988.
56. van Eden W, van der Zee R, Prakken B. Heat-shock proteins induce T-cell regulation of chronic inflammation. Nat Rev Immunol 2005;5:318–330.
57. Kamphuis S, Kuis W, de Jager W, Teklenburg G, Massa M, Gordon G, Boerhof M, Rijkers GT, Uiterwaal CS, Otten HG, et al. Tolerogenic immune responses to novel T-cell epitopes from heat-shock protein 60 in juvenile idiopathic arthritis. Lancet 2005;366:50–56.
58. Elst EF, Klein M, de Jager W, Kamphuis S, Wedderburn LR, van der Zee R, Albani S, Kuis W, Prakken BJ. Hsp60 in inflamed muscle tissue is the target of regulatory autoreactive T cells in patients with juvenile dermatomyositis. Arthritis Rheum 2008;58:547–555.
59. Prakken BJ, Samodal R, Le TD, Giannoni F, Yung GP, Scavulli J, Amox D, Roord S, de Kleer I, Bonnin D, et al. Epitope-specific immunotherapy induces immune deviation of proinflammatory T cells in rheumatoid arthritis. Proc Natl Acad Sci USA 2004;101:4228–4233.
60. Raz I, Avron A, Tamir M, Metzger M, Symer L, Eldor R, Cohen IR, Elias D. Treatment of new-onset type 1 diabetes with peptide DiaPep277 is safe and associated with preserved beta-cell function: Extension of a randomized, double-blind, phase II trial. Diabetes Metab Res Rev 2007;23:292–298.
61. Barsheshet A, Barshack I, Keren P, Keren G, George J. Whole-body hyperthermia attenuates experimental autoimmune myocarditis in the rat. Cardiovasc Pathol 2008;17: 375–381.

Journal of Translational Medicine BioMed Central

Research

Open Access

Aberrant expression and potency as a cancer immunotherapy target of alpha-methylacyl-coenzyme A racemase in prostate cancer

Ichiya Honma[1,2], Toshihiko Torigoe*[1], Yoshihiko Hirohashi[1], Hiroshi Kitamura[2], Eiji Sato[2], Naoya Masumori[2], Yasuaki Tamura[1], Taiji Tsukamoto[2] and Noriyuki Sato[1]

Address: [1]Department of Pathology, Sapporo Medical University School of Medicine, Sapporo, Japan and [2]Department of Urology, Sapporo Medical University School of Medicine, Sapporo, Japan

Email: Ichiya Honma - ichiya@sapmed.ac.jp; Toshihiko Torigoe* - torigoe@sapmed.ac.jp; Yoshihiko Hirohashi - hirohash@sapmed.ac.jp; Hiroshi Kitamura - hkitamu@sapmed.ac.jp; Eiji Sato - eiji@sapmed.ac.jp; Naoya Masumori - masumori@sapmed.ac.jp; Yasuaki Tamura - ytamura@sapmed.ac.jp; Taiji Tsukamoto - taijit@sapmed.ac.jp; Noriyuki Sato - nsatou@sapmed.ac.jp

* Corresponding author

Published: 9 December 2009

Journal of Translational Medicine 2009, **7**:103 doi:10.1186/1479-5876-7-103

Received: 29 January 2009
Accepted: 9 December 2009

This article is available from: http://www.translational-medicine.com/content/7/1/103

Abstract

Alpha-methylacyl-CoA racemase (AMACR) is an enzyme playing an important role in the beta-oxidation of branched-chain fatty acids and fatty acid derivatives. High expression levels of AMACR have been described in various cancers, including prostate cancer, colorectal cancer and kidney cancer. Because of its cancer-specific and frequent expression, AMACR could be an attractive target for cytotoxic T-lymphocyte (CTL)-based immunotherapy for cancer. In the present study, we examined the induction of AMACR-specific CTLs from prostate cancer patients' peripheral blood mononuclear cells (PBMCs) and determined HLA-A24-restricted CTL epitopes.

RT-PCR and immunohistochemical analysis revealed that AMACR was strongly expressed in prostate cancer cell lines and tissues as compared with benign or normal prostate tissues. Four AMACR-derived peptides carrying the HLA-A24-binding motif were synthesized from the amino acid sequence of this protein and analyzed to determine their binding affinities to HLA-A24. By stimulating patient's PBMCs with the peptides, specific CTLs were successfully induced in 6 of 11 patients. The peptide-specific CTLs exerted significant cytotoxic activity against AMACR-expressing prostate cancer cells in the context of HLA-A24. Our study demonstrates that AMACR could become a target antigen for prostate cancer immunotherapy, and that the AMACR-derived peptides might be good peptide vaccine candidates for HLA-A24-positive AMACR-expressing cancer patients.

Introduction

Cytotoxic T lymphocytes (CTLs) play a major role in the anti-cancer immune response [1]. Thus far, large numbers of tumor-associated antigens and their CTL epitopes have been identified [2,3]. High-throughput gene expression profiling using a cDNA microarray allows for systematic interrogation of transcriptionally altered genes. By comparing the mRNA expression profiles of cancerous lesions

with non-cancerous lesions, a number of candidate antigens for tumor-specific immunotherapy have emerged. CTL epitope peptides derived from tumor-specific antigens like the MAGE gene family have been employed for pioneering studies of immunotherapy in cases of advanced melanoma patients [4,5].

Castration-resistant prostate cancer is an aggressive disease with limited treatment options. Hence, there is great need for new therapeutic strategies to treat prostate cancer, and recent progress in understanding of tumor immunology has raised expectations that antigen-specific immunotherapy may become a new modality for cancer therapy. Alpha-methylacyl coenzyme A racemase (AMACR) was identified as one of the genes that were highly expressed in prostate cancer tissues through gene expression profiling using a DNA microarray and RT-PCR [6-8]. AMACR is an enzyme that catalyzes the racemization of alpha-methyl carboxylic coenzyme A thioesters in mitochondria and peroxisomes [9,10]. AMACR is expressed abundantly in prostate cancer tissues as well as colorectal cancer and lung cancer tissues, whereas it is barely detected in benign tissues and normal prostate epithelial cells [6-8]. Immunohistochemical staining for AMACR is currently used in the clinical setting to support the histological diagnosis of prostate cancer. Because it has characteristics of cancer-specific expression and frequent expression in various cancers, AMACR is an attractive target for cancer immunotherapy. In the present study, we examined the induction of AMACR-specific CTLs from prostate cancer patients' peripheral blood mononuclear cells (PBMCs) and determined HLA-A24-restricted CTL epitopes. Our study demonstrates for the first time HLA-A24-restricted AMACR-derived CTL epitopes that might be suitable for peptide vaccines for AMACR-expressing cancer patients.

Materials and methods

Tissue Samples and PBMC

Surgically resected tissue specimens and PBMCs were obtained from HLA-A*2402-positive prostate cancer patients who were treated at Sapporo Medical University Hospital (Sapporo, Japan) after obtaining their informed consent. The study was approved by the Institutional Review Board for Clinical Research at our university. The expression of HLA-A24 molecules on PBMCs of cancer patients was determined by flow cytometry using an anti-HLA-A24 monoclonal antibody (c7709A2.6, kindly provided by Dr. P. G. Coulie, Ludwig Institute for Cancer Research, Brussels Branch).

Cell Lines and Culture

Prostate cancer cell lines (LNCaP, DU145, and PC-3) and proerythroleukemia cell line K562 were cultured in RPMI 1640 (Sigma, St. Louis, MO) supplemented with 10% fetal bovine serum (FBS) (Filtron, Brooklyn, Australia). T2-A*2402 cells, which are transporters associated with antigen processing (TAP)-deficient T2 cells transfected with HLA-A*2402 complementary DNA (cDNA) were cultured in RPMI 1640 supplemented with 10% fetal bovine serum and 800 I g/mL G418 (Invitrogen Life Technologies Co., Carlsbad, CA). LNCaP and DU145 are HLA-A*2402-negative prostate cancer cell lines. To generate LNCaP and DU-145 sublines expressing HLA-A24, HLA-A*2402 cDNA was transduced into the cells by electroporation using a Gene Pulser (Bio-Rad, Richmond, CA) as reported previously [11]. The expression of HLA-A24 molecules on the cell lines was determined by flow cytometry using the anti-HLA-A24 monoclonal antibody. LNCaP-A*2402 and DU145-A*2402, stable HLA-A*2402 transfectants of LNCaP and DU145 cells, respectively, were established and cultured in RPMI 1640 supplemented with 10% FBS and 500 ng/ml puromycin (Sigma).

Reverse transcriptase-polymerase chain reaction (RT-PCR)

Multiple Tissue cDNA Panels (BD Biosciences Clontech, Palo Alto, CA) were used as a template of normal tissue cDNA. Total RNA was extracted using an RNeasy kit (Qiagen, Hilden, Germany). A cDNA mixture was synthesized from 1 I g of total RNA by reverse transcription (RT) using Superscript II and oligo (dT) primer (Invitrogen Life Technologies) according to the manufacturer's protocol. PCR amplification was done in 50 I L of PCR mixture containing 1 I L of the cDNA mixture, 1 I L of KOD Plus DNA polymerase (TOYOBO, Osaka, Japan) and 15 pmol of primers. For specific detection of AMACR, forward primer 5'-CGG GGT ACC ATG GCA CTG CAG GGC ATC TCG-3' and reverse primer 5'-ATA AGA ATG CGG CCG CGA GAC TAG CTT TTA CCT TAT TAC T-3' were employed. As an internal control, ∩-actin expression was detected by using forward primer 5'-ACT GGC TCG TGA TGG ACT C-3' and reverse primer 5'-TCA GGC AGC TCG TAG CTC TT-3'. The amplification protocol consisted of denaturation for 15 seconds at 98°C, annealing for 45 seconds at 58°C and extension for 4 minutes at 72°C for a total of 30 cycles, using a GeneAmp PCR system model 2400 (Perkin-Elmer, Foster City, CA).

Immunohistochemical Staining of Tissue Sections

Immunohistochemical staining was done with formalin-fixed paraffin-embedded tissue sections of surgically resected prostate cancer specimens. Four- to 5-I m-thick sections were deparaffinized in xylene and rehydrated in graded alcohols. Antigen retrieval was done by boiling sections for 20 minutes in a microwave oven in preheated 0.01 mol/L sodium citrate buffer (pH 6.0). Endogenous peroxidase activity was blocked by 3% hydrogen peroxide in ethanol for 10 minutes. After blocking with 1% non-fat dry milk in phosphate-buffered saline (PBS) (pH 7.4), the

sections were reacted with a rabbit polyclonal antibody to AMACR (clone RP134, Diagnostic BioSystems Co., Pleasanton, CA, USA) at 25 I g/mL or preimmune sera for 1 hour, followed by incubation with biotinylated goat anti-rabbit IgG (Nichirei, Tokyo, Japan) for 30 minutes. Subsequently, the sections were stained with streptavidin-biotin complex (Nichirei), followed by incubation with 3,3-diaminobenzidine and counterstaining with hematoxylin. The same tissues were immunostained with an anti-prostate-specific antigen (PSA) polyclonal antibody (DAKO, Denmark).

Peptides and Cytokines

AMACR-derived peptides were synthesized from the amino acid sequence of AMACR based on the HLA-A24-binding motifs. AMACR-derived peptides were provided by Dainippon Sumitomo Pharmaceutical Co. (Osaka, Japan). Two peptides were used as control peptides, Epstein-Barr virus (EBV) LMP2-derived peptide (TYGPVFMSL) and human immunodeficiency virus (HIV) env-derived peptide (RYLRDQQLLGI), which have been shown to become CTL epitopes in the context of HLA-A*2402 previously [12,13], and ovalbumin-derived SL-8 peptide (OVA257-264, SIINFEKL) was used as a negative control peptide. These peptides were synthesized and purchased from Sigma Genosys (Ishikari, Japan). The peptides were dissolved in DMSO at a concentration of 5 mg/mL and stored at -80°C. Human recombinant interleukin (IL)-2, IL-4 and granulocyte macrophage colony-stimulating factor (GM-CSF) were kind gifts from Takeda Pharmaceutical Co. (Osaka, Japan), Ono Pharmaceutical Co. (Osaka, Japan) and Novartis Pharmaceutical (Basel, Switzerland), respectively. Human recombinant IL-7 was purchased from Invitrogen Life Technologies.

Peptide Binding Assay

Peptide binding affinity to the HLA-A24 molecule was assessed by HLA-A24 stabilization assay as described previously [13], based on the findings that MHC class I molecules could be stabilized on the cell surface in the presence of binding peptides. After incubation of T2-A*2402 cells in culture medium at 26°C for 18 hours, the cells (2×10^5) were washed with PBS and suspended with 1 mL of Opti-MEM (Life Technologies) with or without 100 I g of peptide, followed by incubation at 26°C for 3 hours and then at 37°C for 3 hours. After washing with PBS, the cells were incubated with the anti-HLA-A24 monoclonal antibody at 4°C for 30 minutes, followed by incubation with fluorescein isothiocyanate (FITC)-conjugated rabbit anti-mouse IgG at 4°C for 30 minutes. The cells were then suspended with 1 mL of PBS containing 1% formaldehyde, and analyzed by FACScan (Becton Dickinson, Mountain View, CA). Binding affinity was evaluated by comparing mean fluorescence intensity (MFI) of HLA-A24 expression in the presence of peptide pulsation to MFI in the absence of the peptide.

Peptide-specific CTL Induction with Immature Dendritic Cells and Phytohemagglutinin Blasts

PBMCs were isolated from prostate cancer patients by standard density gradient centrifugation on Lymphoprep (Nycomed, Oslo, Norway). PBMCs were incubated in AIM-V medium (Invitrogen Life Technologies, Inc.) supplemented with 2-mercaptoethanol (50 I M) and HEPES (10 mM) for 2 hours at 37°C in a culture flask to separate adherent cells and non-adherent cells. Adherent cells were then cultured in the presence of IL-4 (1000 units/ml) and GM-CSF (1000 units/ml) in AIM-V medium for 7 days to generate monocyte-derived dendritic cells (DCs). The adherent cells containing DCs and phytohemagglutinin (PHA)-stimulated blasts were used as antigen-presenting cells (APCs). CD8-positive T lymphocytes were isolated from non-adherent cells with the MACS separation system (Milteny Biotech, Bergish Blabach, Germany) using an anti-CD8 monoclonal antibody coupled with magnetic microbeads according to the manufacturer's instructions. To obtain PHA-stimulated blasts, CD8-negative non-adherent PBMCs were cultured in AIM-V medium containing 1 I g/ml PHA (WAKO Chemicals, Osaka, Japan) and 100 units/ml of IL-2 for 3 days, followed by washing and cultivation in the presence of IL-2 (100 units/ml) for 4 days.

CTLs were induced from PBMCs of cancer patients by using autologous DC and PHA-blasts as APCs as described previously [14,15]. Briefly, APCs were cultured in AIM-V medium supplemented with 50 I mol/L peptide at room temperature for 2 hours, followed by washing with AIM-V once, then irradiated (100 Gy) and used for stimulation of CTLs. The CTL induction procedure was initiated by stimulating $CD8^+$ cells with peptide-pulsed autologous DCs at a 20:1 effector/APC ratio in AIM-V supplemented with HEPES, 2-ME, and IL-7 (10 ng/mL) for 7 days at 37°C. The following stimulation was done with peptide-pulsed PHA-blasts at a 10:1 effector/APC ratio. On the day after the 2nd stimulation, IL-2 was added to the culture at a concentration of 10 units/mL. The same CTL stimulation cycle with PHA-blasts was then done twice more over a period of 2 weeks. One week after the 4th stimulation, cytotoxic activity of the CTL was measured by ^{51}Cr release assay.

Cytotoxicity Assay

The cytotoxic activities of CTLs were measured by ^{51}Cr-release assay as described previously [16]. Target cells were labeled with 100 I Ci of ^{51}Cr for 1 hour at 37°C and washed with RPMI 1640 three times. Then ^{51}Cr-labeled target cells were incubated with or without peptide and effector cells at various effector/target ratios at 37°C for 6

hours in V-bottomed 96-well microtiter plates. Then supernatants were collected and the radioactivity was measured with a gamma-counter. The % specific lysis was calculated as follows: % specific lysis = (test sample release - spontaneous release) × 100/(maximum release - spontaneous release). For peptide-pulsed target cells, T2-A*2402 cells were incubated with 1 I g/ml peptide at room temperature for 1 hour before the assay. Moreover, we also examined cytotoxic activity against LNCaP, LNCaP-A*2402, DU145 and DU145-A*2402 prostate cancer cells, which express endogenous AMACR.

ELISPOT Assay

ELISPOT plates were coated sterilely overnight with an IFN-Bcapture antibody (Beckton Dickinson Biosciences) at 4°C. The plates were then washed once and blocked with AIM-V medium containing 10% human serum for 2 hr at room temperature. CD8-positive T cells separated from patients' PBMCs (5×10^3 cells/well), which were stimulated in vitro with peptides, were then added to each well along with HLA-A24-transfected CIR cells (CIR-A24) (5×10^4 cells/well), which had been preincubated with the AMACR peptide (10 I g/ml) or HIV peptide as a negative control. After incubation in a 5% CO_2 humidified chamber at 37°C for 24 hours, the wells were washed vigorously five times with PBS and incubated with a biotinylated anti-human IFN-B antibody and horseradish peroxidase-conjugated avidin. Spots were visualized and analyzed using KS ELISPOT (Carl Zeiss, Germany).

Statistical Analysis

We tested the statistical significance of cytotoxic activity of CTLs induced with peptides using Student's t-test. A value of $p < 0.05$ was considered to indicate statistical significance.

Results

AMACR Expression in Normal Tissues, Prostate Cancer Cell Lines and Cancer Tissues

First the expression profile of AMACR in normal adult tissues by RT-PCR was difined. We detected the overt expression of ∩actin mRNA and AMACR mRNA in prostate cancer line LNCaP, but only very weak expression of AMACR mRNA was observed in normal adult liver and pancreas (Figure 1A). In contrast, the AMACR mRNA level was elevated in all three prostate cancer cell lines (LNCaP, DU145 and PC-3) and in surgically resected prostate cancer tissues (Figure 1B and 1C). Low levels of expression were detected in non-cancerous prostate tissues (Figure 1C).

Immunohistochemical analysis revealed that AMACR was present in prostate cancer tissues in 27 (69.2%) of the 39 patients (Figures 2A and 2B). AMACR was weakly detected in non-cancerous prostate tissues, but barely detected in normal essential tissues such as adult liver and pancreas by immunohistochemical staining. In contrast, PSA was stained in both prostate cancer tissue and non-cancerous tissue (Figure 2C). These data indicated that AMACR had a mostly cancer-specific expression profile at both the mRNA level and protein levels.

AMACR-derived Peptides Carrying HLA-A24 Binding Motif

Antigenic peptides derived from AMACR protein might be presented by HLA class I molecules and recognized by CD8-positive T cells. We focused on HLA-A*2402-restricted peptides because of its high frequency in Asian people. The amino acid sequence of AMACR protein was screened for peptides that had an HLA-A24 binding motif, such as 9- and 10-mer peptides with Y, F, M, or W at the 2nd position and L, I, F, or M at COOH-terminal position [17]. Consequently, we found four peptides, AMACR1 (NYLALSGVL), AMACR2 (NMVEGTAYL), AMACR3 (FYELLIKGL) and AMACR4 (IYQLNSDKII) carrying the HLA-A24 binding motif (Figure 3A). Next, we assessed their binding affinities to HLA-A24 molecules by a binding assay using TAP-deficient T2 cells transfected with HLA-A*2402. The MFI of cell surface HLA-A24 was clearly increased in the presence of positive control peptides, EBV peptide and HIV peptide, whereas it was not changed in the presence of negative control peptide SL-8, indicating the adequate qualification of this assay. The HLA-A24 level on the cell surface of T2-A*2402 cells was up-regulated in the presence of AMACR1, AMACR2 and AMACR3 peptides, but not in the presence of AMACR4 peptide, indicating that AMACR1, 2 and 3 peptides were possible HLA-A24-presentable peptides (Figure 3B).

CTL Induction from PBMCs of HLA-A24-positive Prostate Cancer Patients

We attempted to induce AMACR peptide-specific CTLs from PBMCs of HLA-A24 positive prostate cancer patients and assessed their cytotoxic activity. PBMCs were cultured with APCs pulsed with a mixture of three AMACR-derived peptides. After stimulation four times with the peptides, the cytotoxic activity against peptide-pulsed target cells was examined by ^{51}Cr-release assay. The CTLs induced by the *in vitro* stimulation with AMACR peptides showed specific reactivity to the peptide-pulsed T2-A*2402 cells in 6 of 11 cases of HLA-A24-positive patients with AMACR-positive prostate cancer (Table 1 and Figures 4, 5, 6 and 7). CTLs could not be induced in any of the patients with AMACR-negative prostate cancer. In five cases (cases 1, 2, 3, 5 and 6) with AMACR-positive prostate cancer, CTLs reacting to AMACR2 peptide-pulsed T2-A*2402 cells were induced (Figure 5). With respect to AMACR1 and the 3 peptides, peptide-specific CTLs were induced in three cases (cases 4, 5 and 6, Figure 4) and two cases (cases 5 and 6, Figure 6), respectively. Since the cytotoxic activity of CTLs of case 6 was relatively low as compared with the

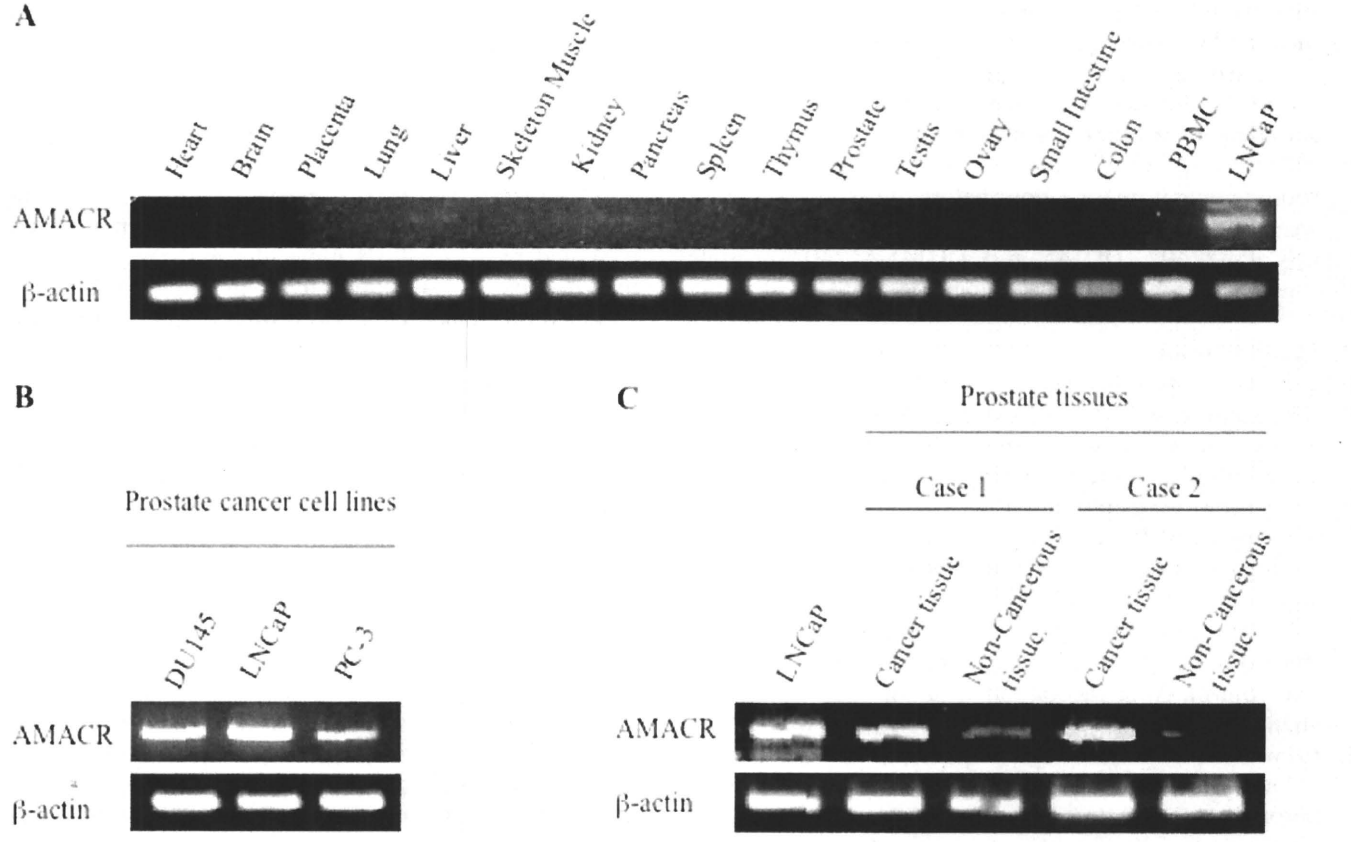

Figure 1
Expression profiles of AMACR as assessed by RT-PCR. A. Expression of AMACR in normal tissues including heart, brain, placenta, lung, liver, skeletal muscle, kidney, pancreas, spleen, thymus, prostate, testis, ovary, small intestine, colon and PBMC. LNCaP, a prostate cancer cell line was used as a positive control for AMACR expression. B. Expression of AMACR in prostate cancer cell lines. Beta-actin expression was detected as an internal control. AMACR mRNA was detected in three prostate cancer cell lines (LNCaP, DU145 and PC-3). C. Expression of AMACR in cancer tissues and noncancerous tissues from surgical specimens of two prostate cancer cases.

other cases, peptide-specificity was assessed by ELISPOT assay. CTLs of case 6 could release interferon-Bin response to AMACR1, 2 and 3 peptides, but not in response to AMACR4 peptide or HIV peptide (Figure 7), indicating that the peptide specificity of the CTLs was consistent with the cytotoxic assay.

Cytotoxic Activity of AMACR Peptide-specific CTLs Against HLA-A24-positive AMACR-positive Prostate Cancer Cell Lines

To confirm that CTLs induced with AMACR peptides could exert cytotoxicity against AMACR-expressing prostate cancer cell lines in an HLA-A*2402-restricted manner, we examined their cytotoxic activity against prostate cancer cell lines that express endogenous AMACR by ^{51}Cr-release assay. LNCaP-A*2402 and DU145-A*2402, which express both endogenous AMACR and gene-transfected HLA-A*2402, were used as target cells. Parental LNCaP and DU145 cells, HLA-A*2402-negative prostate cancer cells, were used as negative control target cells. As shown in Figure 8, CTLs induced from PBMCs of HLA-A*2402-positive prostate cancer patients (cases 3, 4 and 5) with AMACR peptides exerted cytotoxic activity against LNCaP-A*2402 and DU145-A*2402 cells but not against LNCaP and DU145 cells. These data implied that the peptide-specific CTLs were capable of recognizing endogenously processed AMACR-derived peptides in an HLA-A24-restricted manner.

Discussion

Specific immunotherapy for cancer is anticipated to become an alternative or complementary therapy for recurrent or metastatic disease. Successful immunotherapy depends on the identification of cancer-specific